Universitat Autònoma de Barcelona

Master project:

Shaping magnetic fields with superconductor-metamaterial hybrids

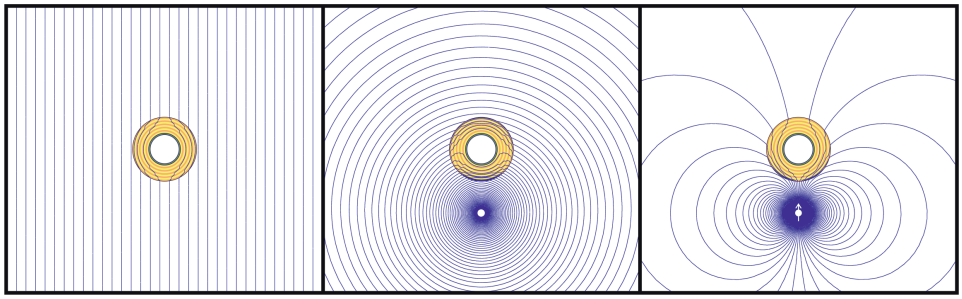

Author:
Jordi Prat Camps

Supervisors:
Carles Navau
Àlvar Sánchez

Bellaterra, 6th July 2011

Els meus agraïments més sincers als tutors d'aquest treball; el Carles i l'Àlvar així com a la resta de membres del grup d'electromagnetisme de la UAB: el Chen, la Nuria, el Guillem i el Sebastià.

També als meus amics, els de Manresa així com tots els que he fet al llarg d'aquests darrers anys de carrera.

I finalment el meu agraïment més profund per les persones més properes a mi: els meus pares Queralt i Toni, el meu germà Marc, avis, oncles i cosins i per la Marina.

Contents

0 Preamble **5**
- 0.1 Summary and motivation . . . 5
- 0.2 Objectives . . . 5
- 0.3 Structure of this work . . . 6

1 Introduction to relevant electromagnetism concepts **7**
- 1.1 Magnetostatics in a medium . . . 7
  - 1.1.1 Linear materials . . . 8
  - 1.1.2 Absence of free currents: magnetic poles densities . . . 8
- 1.2 Maxwell's equations and boundary conditions . . . 8

2 Introduction to metamaterials **11**
- 2.1 Definition of the "metamaterial" concept . . . 11
- 2.2 Brief historical review . . . 11
- 2.3 Mathematical technique to design electromagnetic metamaterials: transformation optics . 14
  - 2.3.1 Application of transformation optics technique to the cylindrical cloaking . . . 15

3 Cylindrical magnetostatic cloaking **19**
- 3.1 Electromagnetics of magnetostatic regime . . . 19
- 3.2 Physical meaning of a magnetostatic cloaking: distortion and detectability . . . 19
  - 3.2.1 Interaction of the magnetic field with a magnetic object: appearance of distortion 20
  - 3.2.2 Distortion as a way to detect the presence of the object . . . 20
  - 3.2.3 Magnetostatic cloaking makes any object magnetically undetectable . . . 21
- 3.3 Permeability tensor that enables magnetostatic cloaking . . . 22

4 Antimagnet design **23**
- 4.1 Rigorous definition of "antimagnet" . . . 23
- 4.2 Homogeneous anisotropic material that enables an approximate cloaking . . . 23
- 4.3 Antimagnet design: discretization of the angular and radial components with two types of feasible layers . . . 26
  - 4.3.1 Tuning process . . . 26
  - 4.3.2 Tuning process for other configurations . . . 28
  - 4.3.3 Evaluation of the antimagnet behavior depending on its specific characteristics . 28
- 4.4 Limitations of the proposed antimagnet designs . . . 30

5 Conclusions **33**

A Validity of the electromagnetic cloaking parameters to obtain magnetostatic cloaking **35**

Bibliography **39**

Chapter 0

Preamble

0.1 Summary and motivation

In this project we present a cylindrically symmetric device that enables magnetostatic invisibility. Although we will rigorous formulate and discuss the meaning of the "invisibility" concept for static magnetic fields, at first it can be thought as a device such that deviates magnetic fields avoiding a certain region without perturbing them outside. The design is initially based on the metamaterial concept and the mathematical technique used to characterize them: transformation optics. From this electromagnetic result we will extract a set of permeabilities (which magnetically characterize any material) that enable magnetic cloaking. In the final part we will discretize our proposal in a series of alternating layers that are already technically available. This will let us propose a feasible device that will make "invisibility" achievable in the magnetostatic regime.

The main motivation for this project has been the large number of pioneering scientific investigations that are directly based on magnetism, in which it is needed an specific control of magnetic fields as in medicine (NMR, for example), functional materials research (for energy transport and generation), matter confinement and others. In fact, the idea of a feasible magnetic cloaking would have not only scientific interest but also important technological applications since magnetic fields are fundamental to many everyday technologies and in many of them it is necessary to have a precise spatial distribution of the magnetic field, which should not be perturbed by magnetic objects - not only by magnets but by any material containing iron or steel, for example. In this context is where we think this work can arouse interest and can make a modest but remarkable step towards a better magnetic fields management with consequences not only in scientific research but also in practical applications.

0.2 Objectives

We summarize the main aims in the following points:

- Present metamaterials field and understand the immense versatility they allow to control electromagnetic fields. Understand and apply a mathematically based technique to design electromagnetic metamaterials that allow an specific control of the electromagnetic fields. Apply this technique to the well known case of cylindrical cloaking.
- Extend the *cloaking* concept to the magnetostatics regime, where there is no time dependence (and there is no electromagnetic induction nor displacement currents). In this context discus and define the meaning of *magnetic field distortion*, *detectability*... to deeply understand what a magnetostatic cloak should do.
- Propose and simulate a magnetic material (characterizen by its permitivity tensor) that enables magnetostatic cloaking. Based on this, outline a feasible design (made of currently available materials) to achieve magnetostatic cloaking and test it by performing numerical simulations. Evaluate its behavior depending on relevant parameters of the design and the applied field.

0.3 Structure of this work

This project has been created following a logical structure that can be summarized in the following points:

1. Introduction to relevant electromagnetism concepts: In this first part we present basic electromagnetic relations and concepts necessary to understand later parts.

2. Introduction to metamaterials: In this part a brief introduction about metamaterials is done. We define the concept and also make a short historical review. We concentrate on a mathematical technique (called *transformation optics*) that lets one determine metamaterial characteristics (material permitivity and permeability tensors) in order to gain a certain control of the electromagnetic fields. We finally apply this to the cylindrical cloaking case.

3. Cylindrical magnetostatic cloak: In this relevant chapter we redefine the meaning of *cloaking* in the magnetostatic context. We explain what magnetic field distortion means and how this can be used to magnetically detect the presence of a material. We also present material parameters necessary to obtain magnetostatic cloaking.

4. *Antimagnet* design: In this final section we start introducing simplified permeabilities (homogeneous but anisotropic) that allow a good approximate magnetic cloaking. Next, we discretize these material parameters proposing a layered structure composed of only two kind of realizable layers. Using numerical simulations and an iterative process permeabilities of layers are tuned leading to the final *antimagnet* design. Antimagnet behavior is studied depending on the number of layers and its permeabilities or the applied magnetic field.

5. Conclusions: We finish the project summarizing the most relevant conclusions extracted from the previous parts.

6. Appendix: Some secondary analytical developments are presented in this final part.

Chapter 1

Introduction to relevant electromagnetism concepts

1.1 Magnetostatics in a medium

The fundamental equations in the magnetostatic regime are [1]

$$\nabla \times \mathbf{H} = \mathbf{J_f}, \tag{1.1}$$
$$\nabla \cdot \mathbf{B} = 0, \tag{1.2}$$

where $\mathbf{H}$ is the *magnetic field*, $\mathbf{B}$ is the *magnetic induction* and $\mathbf{J_f}$ is the *free current density*. These equations lead to the following boundary conditions that fields have to satisfy at the interface between two magnetic media

$$\mathbf{n} \times (\mathbf{H_1} - \mathbf{H_2}) = \mathbf{K_f}, \tag{1.3}$$
$$\mathbf{n} \cdot (\mathbf{B_1} - \mathbf{B_2}) = 0, \tag{1.4}$$

where $\mathbf{K_f}$ is the *free surface current density* and $\mathbf{n}$ is a unitary vector perpendicular to the interface that points outwards medium 2.

The magnetic field and the magnetic induction are related to each other by means of the *magnetization* $\mathbf{M}$ as

$$\mathbf{B} = \mu_0(\mathbf{H} + \mathbf{M}), \tag{1.5}$$

so that when there is no material, fields are simply linked through the vacuum permeability constant μ_0 as $\mathbf{B} = \mu_0\mathbf{H}$. Considering this equations 1.1 and 1.3 can also be rewritten as a function of the magnetic induction as

$$\nabla \times \mathbf{B} = \mu_0(\mathbf{J_f} + \mathbf{J_M}), \tag{1.6}$$
$$\mathbf{n} \times (\mathbf{B_1} - \mathbf{B_2}) = \mu_0(\mathbf{K_f} + \mathbf{K_M}), \tag{1.7}$$

where $\mathbf{J_M}$ and $\mathbf{K_M}$ are the *magnetization current density* and the *magnetization sheet current density*, respectively, defined as

$$\equiv \nabla \times \mathbf{M}, \tag{1.8}$$
$$\mathbf{J_M} \equiv \mathbf{n} \times (\mathbf{M_1} - \mathbf{M_2}). \tag{1.9}$$

Another relevant magnitude is the *magnetic susceptibility tensor* $\chi_m(\mathbf{H}, \mathbf{r})$, defined as

$$\mathbf{M}(\mathbf{r}) = \chi_m(\mathbf{H}, \mathbf{r}) \cdot \mathbf{H}(\mathbf{r}). \tag{1.10}$$

This lets us rewrite equation 1.5 as

$$\mathbf{B}(\mathbf{r}) = \mu_0(\mathbf{1} + \chi_m(\mathbf{H}, \mathbf{r}))\mathbf{H}(\mathbf{r}) = \mu_0 \cdot \mu(\mathbf{H}, \mathbf{r})\mathbf{H}(\mathbf{r}), \tag{1.11}$$

where the *magnetic permeability tensor* has been defined as $\mu(\mathbf{H}, \mathbf{r}) \equiv \mathbf{1} + \chi_m(\mathbf{H}, \mathbf{r})$.

If the currents distribution along the whole space is known we can calculate magnetic induction field inside and outside the material as

$$\mathbf{B}(\mathbf{r}) = \frac{\mu_0}{4\pi} \int_V (\mathbf{J_f}(\mathbf{r}') + \mathbf{J_M}(\mathbf{r}')) \times \frac{\mathbf{r} - \mathbf{r}'}{|\mathbf{r} - \mathbf{r}'|^3} dV'. \tag{1.12}$$

If material is characterized by its permeability $\mu(\mathbf{H}, \mathbf{r})$ the rest of magnitudes can be found using expression 1.11 to determine magnetic field $\mathbf{H}$ and 1.5 to find the magnetization $\mathbf{M}$ (knowing that outside the material $\mu = 1$ and $\mathbf{M} = 0$).

1.1.1 Linear materials

The general relation 1.10 can be simplified if we assume that magnetic materials are linear. Along this project we will always assume this simplification so that we can rewrite equations 1.10 and 1.11 as

$$\mathbf{M}(\mathbf{r}) = \chi_m(\mathbf{r})\mathbf{H}(\mathbf{r}), \tag{1.13}$$

$$\mathbf{B}(\mathbf{r}) = \mu_0(\mathbf{1} + \chi_m(\mathbf{r}))\mathbf{H}(\mathbf{r}) = \mu_0\mu(\mathbf{r})\mathbf{H}(\mathbf{r}), \tag{1.14}$$

respectively. In this case susceptibility $\chi(\mathbf{r})$ and permeability $\mu(\mathbf{r})$ are tensorial magnitudes whose elements only depend on the position.

1.1.2 Absence of free currents: magnetic poles densities

When the *free current density* $\mathbf{J_f}$ is 0 equation 1.1 can be written as

$$\nabla \times \mathbf{H} = 0, \tag{1.15}$$

meaning that magnetic field can be expressed as minus the gradient of a scalar magnitude that we call *magnetic scalar potential* Φ_m. This establishes a perfect analogy with the electrostatic case and this lets us understand magnetic field $\mathbf{H}$ as the sum of the *external applied field* $\mathbf{H_a}$ and the *demagnetizing field* $\mathbf{H_d}$

$$\mathbf{H} = \mathbf{H_a} + \mathbf{H_d}. \tag{1.16}$$

In this case demagnetizing field is the field created by the *surface* (σ_M) and *volume magnetic poles densities* (ρ_M), defined as

$$\sigma_M = \mathbf{M} \cdot \mathbf{n}, \tag{1.17}$$

$$\rho_M = -\nabla \cdot \mathbf{M}, \tag{1.18}$$

where $\mathbf{n}$ is the normal unit vector perpendicular to the surface. Finally, demagnetizing field $\mathbf{H_d}$ can be calculated using magnetic poles densities as

$$\mathbf{H_d}(\mathbf{r}) = \frac{1}{4\pi} \int_V \rho_M(\mathbf{r}') \frac{\mathbf{r} - \mathbf{r}'}{|\mathbf{r} - \mathbf{r}'|^3} dV' + \frac{1}{4\pi} \int_S \sigma_M(\mathbf{r}') \frac{\mathbf{r} - \mathbf{r}'}{|\mathbf{r} - \mathbf{r}'|^3} dS'. \tag{1.19}$$

The main difficulty of this approach is that $\mathbf{H_d}$, σ_M, ρ_M and $\mathbf{M}$ are linked in a complex way; because $\mathbf{H_d}$ depends on σ_M and ρ_M (1.19) which depend on $\mathbf{M}$ (1.17, 1.18) but at the same time magnetization depends on $\mathbf{H_d}$ (1.10, 1.16) too. To solve this problem several strategies can be followed. A basic option to numerically solve it is to use an iterative method.

1.2 Maxwell's equations and boundary conditions

Electromagnetism is fully described by the electric and magnetic constitutive relations (which relate $\mathbf{B}$ with $\mathbf{H}$ (eq. 1.10) and $\mathbf{D}$ with $\mathbf{E}$), the Lorentz's force equation plus the four Maxwell's equations :

$$\nabla \times \mathbf{E} = -\frac{\partial \mathbf{B}}{\partial t}, \tag{1.20}$$

$$\nabla \times \mathbf{H} = \mathbf{J_f} + \frac{\partial \mathbf{D}}{\partial t}, \tag{1.21}$$

$$\nabla \cdot \mathbf{D} = \rho_f, \tag{1.22}$$

$$\nabla \cdot \mathbf{B} = 0, \tag{1.23}$$

where $\mathbf{E}$ is the *electric field* and $\mathbf{D}$ the *displacement field*. The way these equations are written in 1.20-1.23 make them valid in any medium [2]. If we are in empty space they can be simplified using electric and magnetic constitutive relations.

From these Maxwell's equations one can derivate boundary conditions equations that electric and magnetic fields must fulfill in each interface that separates two media:

$$\mathbf{n} \times (\mathbf{E_1} - \mathbf{E_2}) = 0, \tag{1.24}$$

$$\mathbf{n} \times (\mathbf{H_1} - \mathbf{H_2}) = \mathbf{K_f}, \tag{1.25}$$

$$\mathbf{n} \cdot (\mathbf{D_1} - \mathbf{D_2}) = \sigma_f, \tag{1.26}$$

$$\mathbf{n} \cdot (\mathbf{B_1} - \mathbf{B_2}) = 0, \tag{1.27}$$

where $\mathbf{n}$ is a unitary vector perpendicular to the interface that points outwards medium 2, $\mathbf{K_f}$ is the surface free current density in the interface and σ_f is the surface free charge density in that surface.

Chapter 2

Introduction to metamaterials

2.1 Definition of the "metamaterial" concept

Metamaterial concept is really new. It was used for the first time in 1999 by professor Rodger M. Walser from Texas University to refer to "macroscopic composites having a synthetic, three-dimensional, periodic cellular architecture designed to produce an optimized combination, not available in nature, of two or more responses to specific excitation" [3]. An alternative definition [4] that gives a more intuitive idea of this concept describes the metamaterial as "a material that owes its properties mainly to its microstruture more than to its composition". Certainly both definitions provide relevant information about the concept, but we will take as a final definition the following:

Electromagnetic metamaterials are materials constituted by an artificial micro-structure that bring them an electromagnetic effective behavior different from what is found in nature.

From this definition [5] several points must be carefully discussed. In the first place we note that a metamaterial is made of small structures and these structures determine its interesting electromagnetic properties [6]. These properties are determined as a macroscopic *effective* behavior (fully characterized by its permitivity and permeability tensors) which can be understood as an average of the responses given by all small structures forming the material. If the metamaterial electromagnetic behavior is understood as this average it is clear that constituting microstructures cannot have arbitrary sizes and there has to exist a characteristic scale. And that is what defines the *effective homogeneity limit* [5] which requires that constituting structures size has to be much smaller than the electromagnetic wavelength (λ). In order to fix ideas we will take this homogeneity limit (p) such that $p < \lambda/4$. This means that if this scale condition is fulfilled and all metamaterial constituting structures are smaller than the *effective homogeneity limit* the substance behaves as if it was homogeneous (because the electromagnetic wave does not appreciate structure details) and it can be fully characterized by its macroscopic effective constitutive parameters.

It is worth to say that the relationship between a certain microstructure and its corresponding effective macroscopic constitutive parameters can be extremely complex and, in general, strongly depends on the frequency of the wave. In the radio-frequency context, microstructure design process requires a deep knowledge of resonance phenomena and results in a challenging engineering and physical task that is beyond the scope of this project.

Nevertheless most of these difficulties related to microstructure design disappear in static conditions. In this case (understood as the limit when frequency tends to zero) associated wavelength becomes infinite, so that there is no *effective homogeneity limit* and therefore it does not exist an upper limit to the size of the constitutive structures.

2.2 Brief historical review

Although the metamaterial concept did not appeared until the 90's some underlying ideas had already been proposed and discussed since long time before. In this section we will make a brief revision of these

first concepts related to the metamaterials field and we will rapidly outline most relevant steps that have led to the currently success of this discipline.

To start we have to look back until 1968, when V. G. Veselago published an article [7] in which he explained the surprising properties that would exhibit a material having simultaneously negative permitivity and permeability. Although this is considered the conceptual seed of the metamaterials field some previous works done by Russian researchers in the 50's had already explored these fields of *negative refraction media* and *backward-wave media* [8, 9, 10].

During the 60's there were developed several structures that enabled backward-wave propagation for microwaves tubes [11, 12, 13]. Also in this period negative refraction was discovered in periodic media [14]. However it was Veselago [7] who synthesized most of these ideas. In this article he exposed a systematic study of the electromagnetic behavior that a material with simultaneously negative permitivity and permeability would have. He called them *left-handed media* (LHM), because of the fact that the electric field vector $\mathbf{E}$, the magnetic field vector $\mathbf{B}$ and the wave vector $\mathbf{k}$ would form a left-handed triad (the vectorial product of the first two would point in the opposite direction of the third). This would mean an interesting difference respect to systems with positive parameters (RHM), because in these systems those three vectors form a right-handed triad (differences can be seen in figure 2.1 a and b).

Apart from this point, Veselago also demonstrated that in such systems several fundamental electromagnetic phenomena would change significantly [5]:

1. Necessary frequency dispersion of the constitutive parameters.
2. Reversal of Doppler effect.
3. Reversal of Vavilov-Cerenkov radiation.
4. Reversal of the boundary conditions relating the normal components of the electric and magnetic fields at the interface between a conventional/right-handed medium (RHM) and a LHM.
5. Reversal of Snell's law.
6. Subsequent negative refraction at the interface between a RHM and a LHM.
7. Transformation of a point source into an exact point image by a LHM slab.
8. Interchange of convergence and divergence effects in convex and concave lenses, respectively, when the lens is made with a LHM.
9. Plasmonic expressions of the constitutive parameters in resonant-type LHM.

Veselago concluded his paper by discussing potential real (natural) "substances" that could exhibit left-handedness. He suggested that "gyrotropic substances possessing plasma and magnetic properties" ("pure ferromagnetic metals or semiconductors"), "in which both ε and μ are tensors" (anisotropic structures), could possibly be LHM. However, he recognized, "Unfortunately, ... , we do not know of even a single substance which could be isotropic and have $\mu < 0$", pointing out how difficult it seemed to realize a practical LHM structure. No left-handed material was indeed discovered at that time. In fact, this impossibility to find natural materials such that had suitable properties made that metamaterials discipline was largely forgoten by the scientific community for more than 25 years. At the end of the 90's the topic started to attract attention again.

A first revolution on LHM (field that soon was generalized with the appearance of the *metamaterial* term) occurred in 1996 when Pendry et al. realized an artificial electric plasma using a thin-wire structure that exhibited negative permitivity [16] (see figure 2.1 c). Three years later Pendry and his coworkers discovered the artificially magnetic plasma whose permeability was negative[17]. In that work, the well-known split-ring resonators (SRR, shown in figure 2.1 d) were used to achieve the negative magnetic response. These discoveries were presented the same year 1999 in the first PECS (*Photonic and Electromagnetic Crystal Structures*) workshop celebrated in Laguna Beach. In this congress Pendry reported their attempts at designing electric and magnetic metamaterials. David Smith and Shelly Schultz were optimistic about the new materials and went on to manufacture the first negatively refracting substance ever made by combining a negative permitivitty and a negative permeability metamaterial in the same

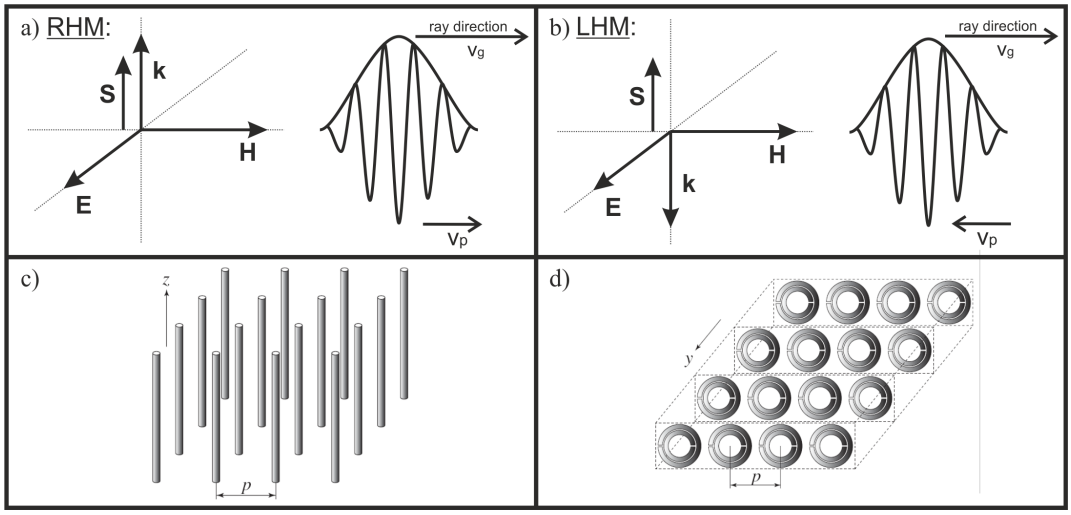

Figure 2.1: Relative distribution of electric field, magnetic field, wave vector and Poynting vector (**S**) in RHM and LHM (a and b respectively). Placement of the first 3 can be directly deduced from Maxwell's equations and implies that in RHM energy propagation direction is the same as the group velocity v_g and the phase velocity v_p. On the other hand in LHM the wave vector **k** has opposite direction so that the phase velocity propagates in the opposite direction of the group velocity and the Poynting vector (these two keep the same direction) [15]. In caption c a thin-wire structure is schemed and in d a group of SRR's.

structure (a combination of wires and SRRs) [18]. The experimental confirmation was presented in 2001 [19]. Their work fired a huge amount of interest, not all of it positive, but the validity of their conclusions has now been confirmed many times over. Their paper opened the way for experimental exploration of Veselago's theoretical concepts.

Inspired by the experimental realization, metamaterials have attracted growing attention in both theoretical exploration and experimental study [20, 21, 22, 23, 24, 25], including the exciting discovery of *perfect lens* and *super lens* [20]. Nowadays these concepts have been not only theoretically studied but also experimentally checked. There have been used silicon carbide structures (which have an effective permitivity near to -1) to get resolutions of $\lambda/20$ [26] (where λ is the wavelength used). However, all these LHM has unavoidable disadvantages of big loss and narrow bandwidth, and such disadvantages have restricted their applications.

In the meantime, an alternative representation of LHM was presented by three groups (Eleftheriades, Oliner and Caloz-Itoh), almost simultaneously in June 2002, using the transmission-line (TL) approach [27, 28, 29, 30, 31, 5]. Without going into details this approach has been used to propose a general *composite right-left-handed* (CRLH) and also to design a lot of microwaves components and antennas [5].

Despite the good properties, LHMs suffer from the large loss and narrow band-width. Hence scientists looked for other features of metamaterial beyond the negative refraction. Then the second revolution on metamaterials discipline came in 2005 when a gradient refractive index medium was realized to bend electromagnetic waves [32]. In the following year a mathematically-based technique called *transformation optics* was presented. This allowed to find material constitutive parameters necessary to execute a precise control of the electromagnetic fields. As an application of this technique there were designed invisibility cloaks using metamaterials [33, 34].

From then on, metamaterials have a much broader meaning than LHM, which do not require the negative permitivity and/or negative permeability, and therefore open a completely new area. After the experimental realization of approximate invisibility cloak in the microwave regime [35, 36], a large explosion of interest has been paid to metamaterials and specially to the transformation optics technique. At the present time there have been designed invisibility cloaks with square shape [37], cylindrical [38], spherical [39] and ellipsoidal [40, 41] but also with more complex shapes [42, 43]. There have also been designed *concentrators* (devices that concentrate electromagnetic fields in a small region of space [37, 44]); EM-field and polarization rotators [45], wave-shape transformers (to design antennas with high gain, for example) [46, 47], EM-wave benders (to reorient electromagnetic waves in the desired direction) [48, 49], and other interesting applications.

Concerning the invisibility topic, recent proposals tend to look for configurations which lead to more realizable material parameters. A recent and successful proposal is called *carpet cloaking*. In the initial article [50] authors proposed that an object sitting on a flat ground plane could be made invisible under a fully dielectric gradient-refractive-index "carpet" cloak generated by conformal mapping. Although this strategy does not lead to strict invisibility (the object must be placed under a carpet and the metamaterial hides the bulge appeared because of the presence of the object) it has significant practical interest because material parameters are not required to have any singularity and, in fact, anisotropy of the cloak can be minimized. Feasibility of this idea has already been experimentally checked [51, 52].

2.3 Mathematical technique to design electromagnetic metamaterials: transformation optics

When we need that electromagnetic fields propagate in a particular way we have to design the metamaterial in such a way that enables this specific control. In principle it could be a difficult job, specially when a non-trivial electromagnetic fields propagation is needed. However, a mathematical technique based on Maxwell's equations form invariance under coordinate transformations makes this task easier and it lets to directly find permitivity and permeability tensors (which are enough to characterize a material from an electromagnetic point of view) that make the desired control possible. This technique is called *transformation optics* [34] and since it was published in 2006 it has been used to theoretically design and characterize innovative devices as electromagnetic cloaks [34, 37] (to deviate electromagnetic waves avoiding a inner region without distorting them outside), concentrators [37, 44] (which concentrate electromagnetic fields in a small region), field and polarization rotators [45], wave-shape transformers [46, 47], and other interesting devices.

Imagine we want light to propagate describing a certain curvature (configuration S'), as it is illustrated in fig 2.2 a. We start from a cartesian coordinates system with simple isotropic and homogeneous permitivity and permeability values (configuration S, illustrated in figure 2.2 b) in which we impose Maxwell's equations to be fulfilled. Then, as we want light to propagate as in S' configuration we proceed to deform the original cartesian coordinate system so that its axis follow the desired curvature. This transformed space is draft in figure 2.2 c (only space inside the dashed rectangle is distorted), and its coordinates (**x'** $= (x', y', z')$) are related with coordinates of original space S ($\mathbf{x} = (x, y, z)$) through a coordinates transformation

$$\mathbf{x}' = \mathbf{x}'(\mathbf{x}) \Rightarrow \begin{cases} x' = x'(x, y, z) \\ y' = y'(x, y, z) \\ z' = z'(x, y, z) \end{cases}, \tag{2.1}$$

and in this transformed space light will propagate describing the desired curvature. However, will Maxwell's equations keep being valid in this transformed space? The answer to this question is affirmative, as long as material parameters rescale properly. This is what we call Maxwell's equations form invariance: if the coordinates system is deformed permitivities and permeabilities must be modified in order to keep Maxwell's equations valid. And this is the key point of this technique, because if we put this new values of permitivity and permeability in a cartesian non-deformed space, fields that will fulfill Maxwell's equations with these new values of μ and ε will be the same that would be if the space was transformed. This means that electromagnetic fields will propagate as if space was deformed, describing the desired curvature (as can be seen in figure 2.2 d).

So thanks to this technique, if we have a certain space transformation described by its corresponding equations (in the form of 2.1), new material parameters μ' and ε' can be calculated by the expressions [34, 4]:

$$\varepsilon'^{i'j'} = [det(\Lambda)]^{-1} \Lambda_i^{i'} \Lambda_j^{j'} \varepsilon^{ij}, \qquad \varepsilon'(\vec{x}') = \frac{\Lambda \cdot \varepsilon(\vec{x}) \cdot \Lambda^T}{det(\Lambda)}, \tag{2.2}$$

$$\mu'^{i'j'} = [det(\Lambda)]^{-1} \Lambda_i^{i'} \Lambda_j^{j'} \mu^{ij}, \qquad \mu'(\vec{x}') = \frac{\Lambda \cdot \mu(\vec{x}) \cdot \Lambda^T}{det(\Lambda)}, \tag{2.3}$$

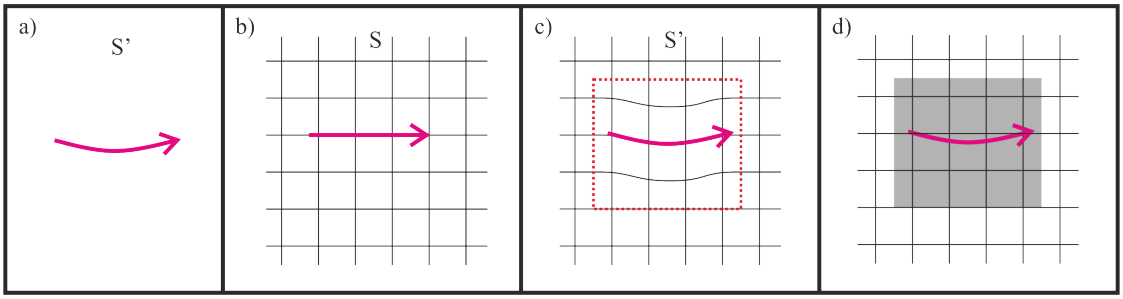

Figure 2.2: Figure a shows the desired light propagation. We start from an empty cartesian non-deformed space (b) where propagation takes places as indicated by the straight arrow. Then we distort space (c) so that propagation in this transformed space describes the desired curvature (only space inside the dashed rectangle has been deformed). Finally we recalculate material parameters that make Maxwell's equations to have the same form in the transformed space [53] and we put these new parameters in the original cartesian non-deformed space so that propagation takes places as if space was effectively deformed.

where:

$$\Lambda_k^{j'} = \frac{\partial x^{j'}}{\partial x^k}. \tag{2.4}$$

Equations 2.2 and 2.3 are expressed in two different but completely equivalent notations. We must advice that these expressions are only valid if coordinate systems are orthogonal [34] (meaning that the sets of unitary vectors in the original and also in the transformed coordinate systems are orthogonal). If it is not the case, it must be followed the whole development explained in [34, 54, 2]. It is worth to remark that this method is more general and it can be applied not only to spacial transformation but also to time-dependent ones [4]. Nevertheless in this project we will only refer to spacial time-independent transformations. Another subtle but important point is that the material parameters calculated using this technique will not cause reflection nor electromagnetic scattering if certain constrains are satisfied. Details can be found in references [55] and [4] but it is enough to know that these materials will not cause scattering nor reflection (i.e. will be useful to get "invisibility") if the coordinates transformation keeps continuity of the transformed space.

2.3.1 Application of transformation optics technique to the cylindrical cloaking

One of the simplest and most powerful devices that can be designed using transformation optics is an "electromagnetic cloak". We define an "electromagnetic cloak" as a shell of material such that avoids electromagnetic fields to enter inside an inner region (meaning that external electromagnetic fields do not interact with any object placed inside) and does not cause any reflection nor scattering outside the device. So that as the incident electromagnetic wave is not modified by the presence of the cloak an external observer would not realize of its presence, achieving invisibility of the device and of any object placed inside.

Although this definition gives freedom to imagine a cloak with an arbitrary geometry (and transformation optics technique can be perfectly applied to design complex geometry cloaks [42, 43]) it is easier to understand and design cloaks with important symmetries in order to obtain simpler material parameters for the cloak. This is the case of *square* [37], *cylindrical* [38], and *spherical* [39] cloaks. In this section we will concentrate on *cylindrical* cloaks, in which its symmetry along z axis (see figure 2.3 a) reduces the problem to 2 dimensions (XY plane).

Assuming this cylindrical symmetry we will apply transformation optics technique to design a cloak that avoids electromagnetic fields to enter inside a radius R_1 . This can be though as a spacial transformation in which we deform space from $r = 0$ to $r = R_2$ compressing and replacing it between $r' = R_1$ and $r' = R_2$ (where $R_2 > R_1$ as can be seen in figure 2.3 b). There are several ways to do this as there exists many ways to compress space between R_1 and R_2. The simplest way to do it is making a linear compression, where a point with radial coordinate r is replaced in a new radial coordinate r' such that the ratio between r and radial distance R_2 is the same as $r' - R_1$ and the shell thickness $R_2 - R_1$. This can be expressed as

$$\frac{r}{R_2} = \frac{r' - R1}{R_2 - R_1} \quad \Longrightarrow \quad r' = \frac{R_2 - R_1}{R_2} r + R_1. \tag{2.5}$$

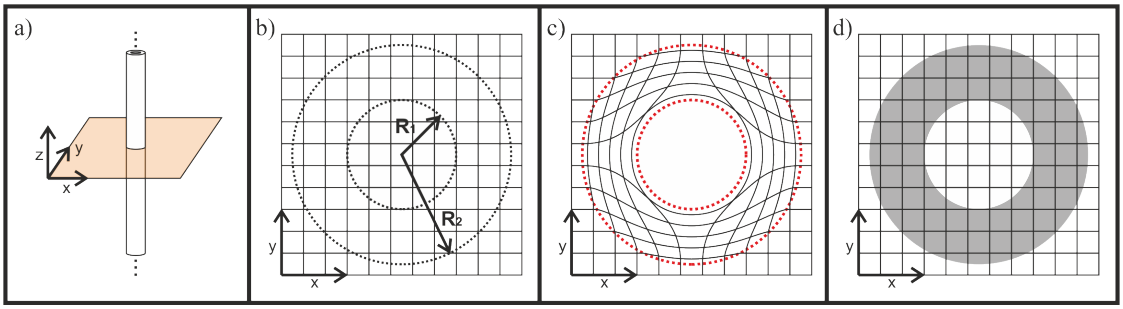

Figure 2.3: Figure a shows the cylindrical symmetry of the system and the relevant xy plane. In b we show inner and outer radius R_1 and R_2 between which we will compress space as is shown in c. Finally in d we indicate the position where the material has to be put in order to cause the same electromagnetic deviation as if the space was effectively deformed like in figure c.

So the complete space transformation is

$$r' = \frac{R_2 - R_1}{R_2} r + R_1, \qquad \phi' = \phi, \qquad z' = z, \qquad r \in (0, R_2] \tag{2.6}$$

$$r' = r, \qquad \phi' = \phi, \qquad z' = z, \qquad r \in (R_2, \infty) \tag{2.7}$$

where primed coordinates r', ϕ', z' refer to the transformed space and r, ϕ, z to the original one, both expressed in the usual cylindrical coordinates system. Doing so transformed space will look like in figure 2.3c (where region inside R_1 contains no space) and material parameters that we will obtain must be placed in coordinates of transformed space (shaded region of figure 2.3 d).

Once the space transformation is outlined, we proceed to find material parameters (μ' and ε') using transformation optics technique. We start with equation 2.4, that determines each element of the transformation matrix Λ. In this equation transformed (x', y', z') and original (x, y, z) spaces are assumed to be cartesian. As our space transformation is expressed in terms of cylindrical coordinates (from cylindrical coordinates system (r', ϕ', z') to (r, ϕ, z)), we must correct some elements of this tensor as follows

$$\Lambda_k^{j'} = \begin{pmatrix} \frac{\partial r'}{\partial x} & \frac{\partial r'}{\partial y} & \frac{\partial r'}{\partial z} \\ r' \frac{\partial \phi'}{\partial x} & r' \frac{\partial \phi'}{\partial y} & r' \frac{\partial \phi'}{\partial z} \\ \frac{\partial z'}{\partial x} & \frac{\partial z'}{\partial y} & \frac{\partial z'}{\partial z} \end{pmatrix}, \tag{2.8}$$

where we have added a multiplying r' factor in the second row. The need of this extra term can be understood if we consider how infinitesimal displacements in cylindrical coordinates are related with the cartesian ones. In figure 2.4 we can see infinitesimal displacements corresponding to r and z coordinate (denoted by **dr** and **dz**) that are vectors obtained by a differential variation of each coordinate. Nevertheless it is very different in the case of the angular coordinate ϕ, where a differential variation of the angle does not has the proper displacement meaning. In this case the infinitesimal displacement vector must be calculated as $\mathbf{r}\mathbf{d}\phi$, as it is shown in figure 2.4 b. And that is the reason why this extra r' term must be added in the second row, when we calculate partial derivatives of the transformed angular coordinate ϕ'. This reasoning must be taken into account whenever angular coordinates are used in order to properly express infinitesimal displacements and to calculate correct partial derivatives.

Following the development, transformation matrix 2.8 can be rewritten as

$$\Lambda_k^{j'} = \begin{pmatrix} \frac{\partial r'}{\partial r}\frac{\partial r}{\partial x} & \frac{\partial r'}{\partial r}\frac{\partial r}{\partial y} & \frac{\partial r'}{\partial r}\frac{\partial r}{\partial z} \\ r' \frac{\partial \phi'}{\partial \phi}\frac{\partial \phi}{\partial x} & r' \frac{\partial \phi'}{\partial \phi}\frac{\partial \phi}{\partial y} & r' \frac{\partial \phi'}{\partial \phi}\frac{\partial \phi}{\partial z} \\ \frac{\partial z'}{\partial z}\frac{\partial z}{\partial x} & \frac{\partial z'}{\partial z}\frac{\partial z}{\partial y} & \frac{\partial z'}{\partial z}\frac{\partial z}{\partial z} \end{pmatrix}. \tag{2.9}$$

Using derivatives chain rule and the fact that r' only depends on r (and obviously ϕ' and z' only depend

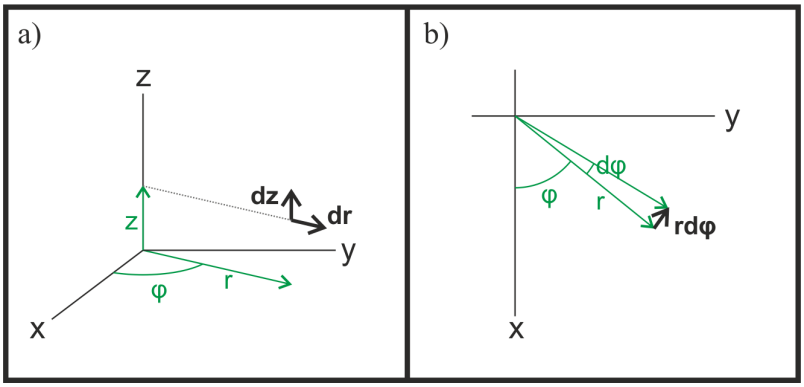

Figure 2.4: Scheme of cylindrical coordinates system and the corresponding infinitesimal displacements.

on ϕ and z respectively). Introducing space transformation equations 2.6 and 2.7, Λ matrix becomes

$$\Lambda_k^{j'} = \begin{pmatrix} \frac{R_2-R_1}{R_2}cos\phi' & \frac{R_2-R_1}{R_2}sin\phi' & 0 \\ r'\frac{R_2-R_1}{R_2(R_1-r')}sin\phi' & r'\frac{R_2-R_1}{R_2(r'-R_1)}cos\phi' & 0 \\ 0 & 0 & 1 \end{pmatrix}. \tag{2.10}$$

All elements are expressed in terms of the transformed space coordinates r', ϕ', z', because we must remember that material parameters μ', ε' have to be placed in transformed space coordinates. Using expressions 2.2 and 2.3 and taking into account that initial space before deformation is an empty cartesian space such that $\mu^{ij} = \varepsilon^{ij} = \delta^{ij}$ we directly find material parameters

$$\mu'^{i'j'} = \varepsilon'^{i'j'} = \begin{pmatrix} \frac{r'-R_1}{r'} & 0 & 0 \\ 0 & \frac{r'}{r'-R_1} & 0 \\ 0 & 0 & \left(\frac{R_2}{R_2-R_1}\right)^2 \cdot \frac{r'-R_1}{r'} \end{pmatrix}, \qquad r' \in (R_1, R_2) \tag{2.11}$$

which are diagonal tensors whose non-zero elements are $\mu_{r'r'} = \varepsilon_{r'r'}$, $\mu_{\phi'\phi'} = \varepsilon_{\phi'\phi'}$ and $\mu_{z'z'} = \varepsilon_{z'z'}$. So the desired permitivity and permeability values are:

$$\boxed{\mu_{r'r'} = \varepsilon_{r'r'} = \frac{r'-R_1}{r'}} \tag{2.12}$$

$$\boxed{\mu_{\phi'\phi'} = \varepsilon_{\phi'\phi'} = \frac{r'}{r'-R_1}} \tag{2.13}$$

$$\boxed{\mu_{z'z'} = \varepsilon_{z'z'} = \left(\frac{R_2}{R_2-R_1}\right)^2 \cdot \frac{r'-R_1}{r'}} \tag{2.14}$$

expressions that can be found in [38]. We can interpret each element of this tensor as the permeability (and permitvity) that the device must have in the radial, angular and z direction (defined by its corresponding infinitesimal displacements $\mathbf{dr}$, $\mathbf{d}\phi$ and $\mathbf{dz}$ shown in figure 2.4) respectively. We already indicated that material parameters must be put in coordinates of the transformed space so that metamaterial have to be displaced in a shell with inner and outer radius R_1 and R_2 respectively. Inside R_1 no material is necessary (and because of this any material we want to hide from electromagnetic fields can be put there) because the space transformation that we have used excluded space from the circular region with radius R_1.

Finally in figure 2.5 a we plot the three material parameters functions respect to the radial coordinate r and in b we show the path that light rays would follow when they interact with such cloaking device.

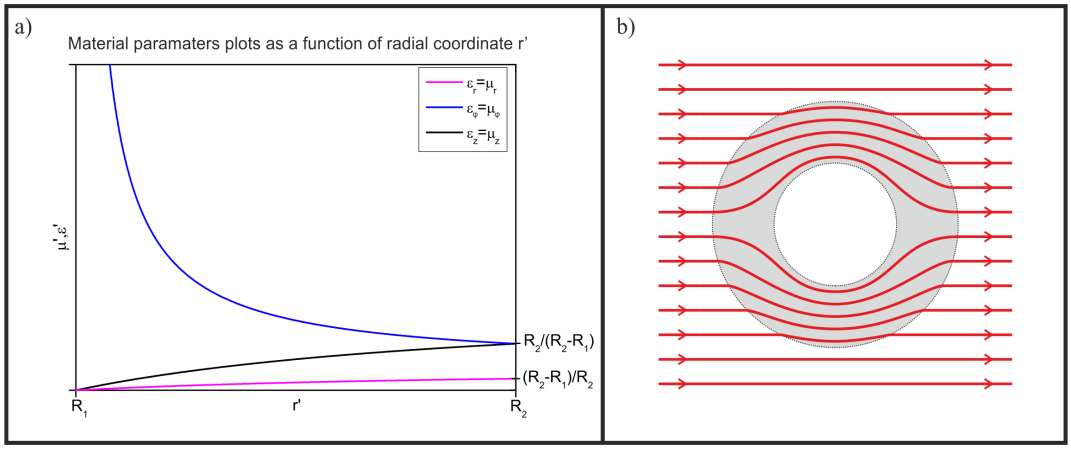

Figure 2.5: In figure a we show plots of material parameters $\mu_{r'r'}$, $\mu_{\phi'\phi'}$ and $\mu_{z'z'}$ as a function of the radial coordinate r'. Notice that angular component diverges in the inner limit $r' = R_1$. In figure b light rays path is schemed, showing how they avoid the central region and how they follow the same path before and after interacting with the cloaking device.

Chapter 3

Cylindrical magnetostatic cloaking

In the previous chapter we have explained and applied a technique called *transformation optics* to find material parameters of a device that allows electromagnetic invisibility of any object placed inside. In this context, *electromagnetic invisibility* can be easily defined as the absence of any absortion, reflection or dispersion of the electromagnetic wave that makes an object electromagnetically detectable. However, if we want to extend this "invisibility" concept to magnetostatic fields some important questions must be reformulated. What does *detectability* mean in a magnetostatic context? What kind of *distortion* appears when a magnetic object is placed in a magnetic field and why does it appear?

In this chapter we will answer these questions and we will extend electromagnetic invisibility concepts to the magnetostatic context.

3.1 Electromagnetics of magnetostatic regime

Maxwell's equations 1.20-1.23 presented in section 1.2 show how electric and magnetic fields are linked not only between them but also to their temporal variation. When we suppose static conditions (i.e. temporal derivatives are zero) electric and magnetic fields become decoupled and this leads to the *electrostatic* and *magnetostatic* regimes. The magnetostatic regime is only ruled by two Maxwell's equations (from eq. 1.21 and 1.23) plus the magnetic constitutive relation (eq.1.14):

$$\nabla \times \mathbf{H} = \mathbf{J_f}, \tag{3.1}$$

$$\nabla \cdot \mathbf{B} = 0, \tag{3.2}$$

$$\mathbf{B} = \mu_0 \mu \mathbf{H}. \tag{3.3}$$

This situation when there is no time dependence of any physical magnitude can be thought as the limit when temporal variations become infinitely slow (this means the case when frequency tends to zero and the wavelength tends to infinity). An infinite associated wavelength implies that there is no scale limit for the size of structures that have to interact with magnetic fields (different from the usual electromagnetic regime, when structures size is delimited by the *effective homogeneity limit*, which depends on the wavelength).

3.2 Physical meaning of a magnetostatic cloaking: distortion and detectability

When we deal with electromagnetic waves the presence of a certain object can be detected due to the appearance of dispersion and absorption phenomena (what makes shadow and different colors to appear as a "visual image"). Nevertheless, in magnetostatics regime we must define another criteria to judge if a certain object can be magnetically detected or not. In the following parts we will define and justify it.

3.2.1 Interaction of the magnetic field with a magnetic object: appearance of distortion

In section 1.1 we have explained the relationship between relevant magnitudes in magnetostatics. We saw that there are different approaches that can be used to describe interaction between magnetic fields and magnetic materials. As we deal with materials in which there are not free currents, from now on we will use the magnetic poles approach (section 1.1.2).

In this framework we need to understand how interaction between magnetic fields and materials take place. To start imagine a certain applied field (for example field created by a magnetic dipole as is sketched in figure 3.1 a). Also imagine an arbitrary magnetic material (with no conductivity and magnetically characterized by its permeability tensor μ). Even thought it has no initial magnetization, when it interacts with applied magnetic field a local magnetization $\mathbf{M}$ will appear in it. As we have explained in section 1.1.2 it causes surface and volume magnetic poles to appear (eqs. 1.17 i 1.18) which create the associated demagnetizing field $\mathbf{H_d}$ (given by eq. 1.19). To calculate magnetic induction $\mathbf{B}$ inside the material we must use the complete equation 1.5. However, outside the material magnetization field $\mathbf{M}$ is zero, so that total magnetic induction will be given by

$$\mathbf{B} = \mu_0(\mathbf{H_a} + \mathbf{H_d}), \tag{3.4}$$

and this equation reflects the key point of interaction between magnetic fields and magnetic materials: the resulting distorted field outside the material is the superposition of the applied induction field ($\mathbf{B_a} = \mu_0\mathbf{H_a}$) and the demagnetizing induction field ($\mathbf{B_d} = \mu_0\mathbf{H_d}$), created by magnetic poles densities (as shown in figure 3.1 c), where the applied dipolar field is drawn in red lines , while demagnetizing field created by magnetic poles densities is drawn in blue lines). The superposition of these two fields is shown in figure 3.1 b). This *demagnetizing field modifies the initial applied field and it is the cause of distortion appearance*.

3.2.2 Distortion as a way to detect the presence of the object

Following the previous development we are ready to understand how the presence of a magnetic material can be detected. We have just seen that the presence of the magnetic object creates a certain demagnetizing field outside that causes distortion of the applied field. But this demagnetizing field also reveals the presence of the magnetic object. For example the magnetic source of the applied field will notice this demagnetizing field so that a certain interaction will appear (because, of course, the source does not notice the field created by itself). If the applied field is created by a dipole, the demagnetizing field created by the magnetic object will, in general, induce a certain torque or a force to this dipole (see scheme of figure 3.1d where is clearly shown this interaction between demagnetizing field and the dipolar source) which will let to detect the object. Another way to realize about the presence of the obtject is doing a precise measure of the total magnetic field that there is in a certain point (near the material). Doing so field that we will measure will be the sum of the applied field (which is known because it only depends on the applied field source and the measuring point) plus the demagnetizing field created by magnetic poles appeared in the magnetic object. Comparing the measured field with the applied field, demagnetizing field can be found, revealing the presence of the object.

If the magnetic object is such that demagnetizing field created by its magnetic poles distribution is zero outside it then the total induction field $\mathbf{B}$ will be the same as the applied induction field $\mathbf{B_a}$, i.e. there will be no field distortion outside and no detection will be possible.

To sum up, in magnetostatics regime we will consider a magnetic object *detectable* if and only if given a certain applied field it becomes modified (outside the object) by the presence of this object.

Finally it is also worth to remark that the demagnetizing field will not only depend on the geometry and the permeability tensor of the object but also on the external applied field, as the appeared magnetic poles densities will depend on it too. This means that distortion caused by a certain object (i.e. its magnetic detectability) will change depending on the magnetic source we use. We must keep this point in mind when we check the magnetic cloaking capability of any device we design.

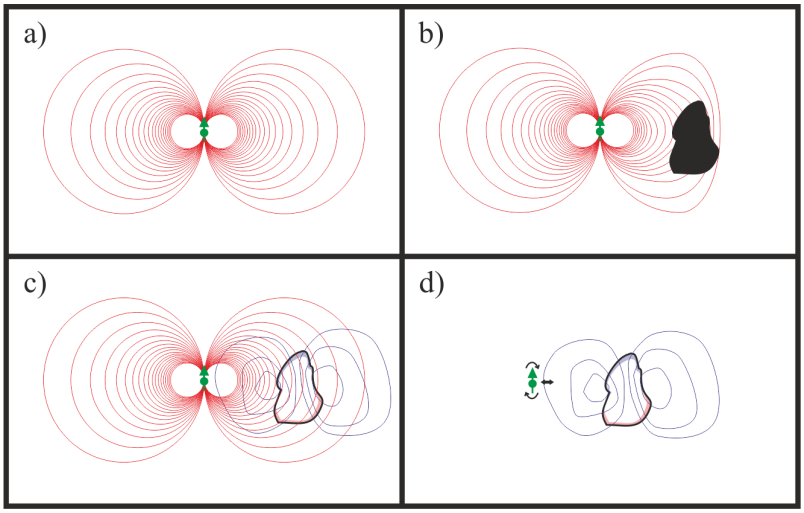

Figure 3.1: Figure a shows applied dipolar field. In b magnetic material (in black) is placed so that magnetic field lines are modified. In figure c we show how this distorted field is the superposition of the demagnetizing field (in blue) and the original dipolar applied field (in red). Demagnetizing field is created by magnetic poles densities appeared in the object. These densities are schemed in figures c and d as red and blue shaded regions inside the material (representing positive and negative poles densities respectively). In figure d interaction between demagnetizing field and the dipole is shown, meaning that the dipole will be aware of the presence of the object.

3.2.3 Magnetostatic cloaking makes any object magnetically undetectable

In the second chapter we described an electromagnetic cloaking device that bends light rays in such a way that they avoid a central region (region where we can put any object we want to hide) and let the rays propagate behind as if the light had traveled in free space (with no absorption nor dispersion, as light rays show in figure 2.5 b).

In this context, a *magnetostatic cloak* [56] makes something completely analogous: it makes magnetic field to avoid a central region leaving the field outside the device undistorted. As there is no distortion outside, the whole device becomes magnetically undetectable and also its content as no external magnetic field reaches the central region. This behavior must be expected for any applied magnetic field in order to guarantee that any magnetic source will not detect its presence (as shown in figure 3.2, where different applied magnetic fields are tested to ensure a perfect undetectably).

Before we conclude this section an interesting discussion must be done. We explained that magnetic poles induced in the material generate a demagnetizing field that causes the applied field distortion and, therefore, allows the object detection. Nevertheless this demagnetizing field naturally decreases its modulus as we go far from the material. This means that at certain distance all magnetic materials become magnetically undetectable (different from what happens with electromagnetic waves, where scattering and absorption phenomena obey different decaying rates). Because of this, any magnetic cloaking device should be evaluated comparing the distortion it generates with the distortion created by another reference material (for example a superconducting or a high permeability ferromagnetic shell).

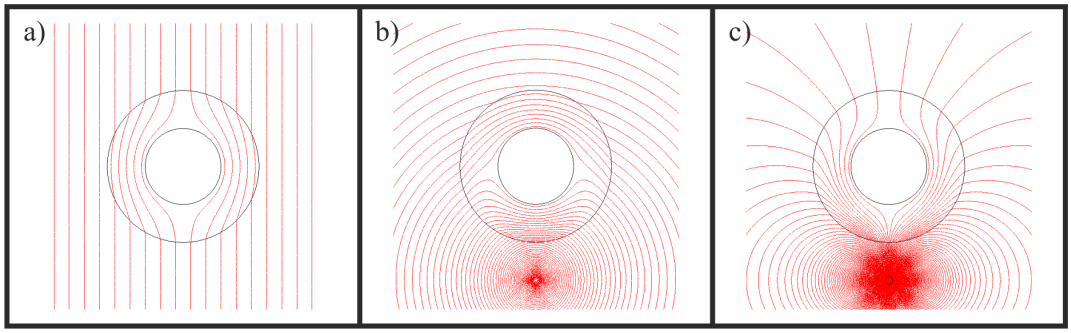

Figure 3.2: Field lines from numerical simulations where different magnetic fields (a: uniform applied field, b: field created by a current wire, c: dipolar field) interact with a cylindrically symmetric cloaking device with permeabilities described by equations 2.12-2.14 taking $R_1 = 0.1m$ and $R_2 = 0.2m$. Outside it there is no distortion in any case so that the device is magnetically undetectable for any magnetic source.

3.3 Permeability tensor that enables magnetostatic cloaking

In principle, tranformation optics technique described in section 2.3 lets us find material parameters (μ' and ε') that make all four Maxwell's equations [2] to be the same in the transformed space and in the real space full of the suitable material. This means that, in principle, this technique should be valid to shape not only the propagation of an electromagnetic wave but also for static magnetic fields (in the magnetostatic regime) and for static electric fields (in the electrostatic regime). Because of this the parameters obtained in section 2.3.1 (expressed in 2.12-2.14) should enable magnetostatic cloaking. Nevertheless, we must be very careful about this affirmation due to the special nature of the space transformation used to obtain cloaking as we have done in section 2.3.1. In this type of transformation we have expanded a infinitesimally thin wire of original space in such a way that it has become a cylinder, whose radius becomes R_1 (we call this a "punctual expansion").

For electromagnetic waves the discussion about the validity of the permeability and permitivity parameters obtained by this space transformation has already been done in [39]. The author justifies that from the perspective of the transformed space the cloaking device would effectively compress the cloaked space (inside R_1) in a infinitely thin line (for cylindrical symmetry) or in an infinitely small sphere (for spherical symmetry). However, in both cases the resulting infinitesimal "line" and "sphere" would not cause dispersion nor reflection of any incident electromagnetic wave, what proves that material parameters obtained by this space transformation are valid in the electromagnetic regime to obtain a perfect cloaking.

Electrostatic and magnetostatic cases, however, have not been discussed yet. And in general, arguments used to demonstrate the validity of parameters for electromagnetic waves do not apply in these regimes. That's why we cannot directly use permitivity parameters found by transformation optics technique (when we have done a "puntual expansion") in the magnetostatics regime expecting the same behavior as with electromagnetic waves. To verify the validity of these parameters we must check magnetic fields behavior in interaction with such device starting from magnetostatic Maxwell's equations (3.1-3.3). For the cylindrically symmetric case this is done in appendix A, where we demonstrate the validity of permeabilities expressed in equations 2.12-2.13 ($\mu_{z'z'}$ parameter expressed in 2.14 is not relevant in the cylindrical magnetostatic case due to the translational symmetry along the z axis) to cloak a uniform applied magnetic field. In addition we have also performed some numerical simulations of this cloaking device interacting with other magnetic sources as a dipole or a current wire. These and the rest of simulations included in this project have been performed using COMSOL Multiphysics software, magnetostatics module. As all devices and fields studied have translational symmetry along the z axis, only bidimensional simulations have been done. In captions from figure 3.2 we can see the results of these simulations which confirm that the device causes null distortion (or less than the numerical resolution of each simulation) for a non-uniform applied field. This shows that quoted permeabilities also cloak static magnetic fields [57].

Chapter 4

Antimagnet design

4.1 Rigorous definition of "antimagnet"

In section 3.2.3 of the previous chapter we already defined the concept of a *magnetostatic cloak* (a device that makes null interior magnetic field and leaves external field undistorted). At this point we want to redefine our goal into a more ambitious one, we want to design an *antimagnet* defined as a material forming a shell that encloses a given region in space while fulfilling the following two conditions:

1. The magnetic field created by any magnetic element inside the inner region (e.g. a permanent magnet) should not leak to outside the region enclosed by the shell.

2. The system formed by the enclosed region plus the shell should be magnetically undetectable from outside for *any* magnetic source (i.e. it has to leave any magnetic field outside the device undistorted).

Since we deal with static magnetic fields we can take advantage that a layer of superconducting material (with $\mu = 0$) at the inner surface would directly fulfill condition (1) [58]. So the main difficulties arise from condition (2) since any superconducting layer would affect the external magnetic field and therefore interact with an external field source. We will solve this problem in two different steps explained in the following two sections.

Feasible antimagnets characterized by these two conditions would have important practical applications both in research and in applied fields. They could be used in experiments in which a precise magnetic field would be needed in order to avoid undesired distortions caused by magnetic materials (not only permanent magnets but also iron-based materials). They could also be used in magnetic resonance tests in order to avoid interaction between the applied magnetic field and ferric parts of the sample (and causing no distortion, so that we still could extract valuable information of the test). It could also have interest in reducing the magnetic signatures of vessels and ferric structures so that they would become magnetically undetectable.

4.2 Homogeneous anisotropic material that enables an approximate cloaking

In section 3.3 we explained that permeabilities expressed in 2.12-2.13 were also valid to build a magnetostatic cloak. Despite of the correct behavior exhibited they are completely impractical because they involve a fine-tuned continuous variation of anisotropic properties. However, can a similar magnetic field behavior (in particular no field distortion in the exterior region) be produced with simpler permeability arrangements? In the following we will demonstrate that a whole family of homogeneous magnetic systems exist with the property that they produce a null effect on an externally applied magnetic field. Each of these systems is a cylindrical shell composed of an homogeneous (i.e. properties are the same in all the material points) anisotropic material.

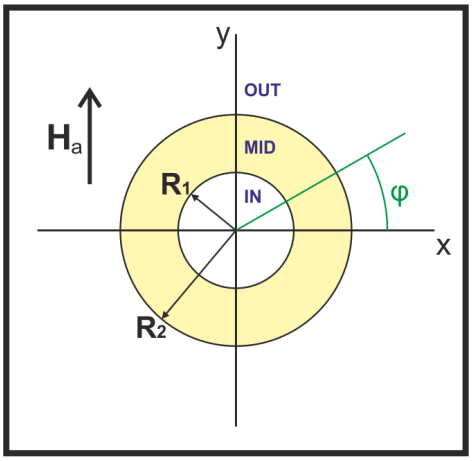

Figure 4.1: Scheme where the three different regions are defined.

Consider one of such cylinders infinitely long along the z axis with radius R_2 and a central coaxial hole of radius $R_1 < R_2$. This cylinder is made of a magnetic material with homogeneous radial and angular relative permeabilities, μ_r and μ_ϕ respectively. A uniform external field $\mathbf{H}_a$ is applied along the y direction. We want to find the analytical expression for the field in all regions ($\mathbf{H}^{out}$, $\mathbf{H}^{mid}$ and $\mathbf{H}^{in}$ as defined in figure 4.1) with the condition that the applied field is not modified by the presence of the cylinder, in the region outside it. We start with the magnetostatic Maxwell's equations 3.1 and 3.2 that must be fulfilled everywhere, in particular inside the material. There, induction and magnetic field components are related through the permeabilities as: $\mathbf{B}_r^{mid} = \mu_0\mu_r\mathbf{H}_r^{mid}$ and $\mathbf{B}_\phi^{mid} = \mu_0\mu_\phi\mathbf{H}_\phi^{mid}$. Using the translational symmetry along the z axis and the fact that there are no free currents nor free charges inside the material magnetostatic Maxwell's equations become

$$H_\phi^{mid} + r\frac{\partial H_\phi^{mid}}{\partial r} - \frac{\partial H_r^{mid}}{\partial \phi} = 0, \tag{4.1}$$

$$\mu_r H_r^{mid} + r\mu_r\frac{\partial H_r^{mid}}{\partial r} + \mu_\phi\frac{\partial H_\phi^{mid}}{\partial \phi} = 0. \tag{4.2}$$

We want to find a solution in which external field is the uniform applied one (so that there is no distortion outside the material) and there is a uniform field inside the hole whose modulus is scaled by a positive factor α ($\mathbf{H}^{in} = \alpha\mathbf{H}_a$):

$$\mathbf{H}_a = H_a\hat{\mathbf{u}}_y = H_a sin\phi\hat{\mathbf{u}}_r + H_a cos\phi\hat{\mathbf{u}}_\phi = H_r^{out}\hat{\mathbf{u}}_r + H_\phi^{out}\hat{\mathbf{u}}_\phi, \tag{4.3}$$

$$\alpha\mathbf{H}_a = \alpha H_a\hat{\mathbf{u}}_y = \alpha H_a sin\phi\hat{\mathbf{u}}_r + \alpha H_a cos\phi\hat{\mathbf{u}}_\phi = H_r^{in}\hat{\mathbf{u}}_r + H_\phi^{in}\hat{\mathbf{u}}_\phi, \tag{4.4}$$

$$\begin{cases} H_r^{out} = H_a sin\phi \\ H_\phi^{out} = H_a cos\phi \end{cases}, \qquad \begin{cases} H_r^{in} = \alpha H_a sin\phi \\ H_\phi^{in} = \alpha H_a cos\phi \end{cases}. \tag{4.5}$$

Then, by imposing continuity of the normal component of $\mathbf{B}$ and the tangential component of $\mathbf{H}$ at the interfaces $r = R_1$ and $r = R_2$ we can express boundary conditions as

$$\begin{cases} H_r^{mid}(r = R_2) = \frac{1}{\mu_r}H_a sin\phi \\ H_\phi^{mid}(r = R_2) = H_a cos\phi \end{cases}, \qquad \begin{cases} H_r^{mid}(r = R_1) = \alpha\frac{1}{\mu_r}H_a sin\phi \\ H_\phi^{mid}(r = R_1) = \alpha H_a cos\phi \end{cases}. \tag{4.6}$$

To solve equations 4.1 and 4.2 with boundary conditions expressed in 4.6 we suppose that solutions can be written as a product of the angular and the radial part

$$\begin{cases} H_r^{mid}(r) = f(r)\frac{1}{\mu_r}H_a sin\phi \\ H_\phi^{mid}(r) = g(r)H_a cos\phi \end{cases}, \tag{4.7}$$

where $f(r)$ and $g(r)$ are arbitrary radially-dependent functions that must be found. By doing so, boundary conditions expressed in 4.6 become

$$\begin{cases} f(r=R_2)=1 \\ g(r=R_2)=1 \end{cases}, \qquad \begin{cases} f(r=R_1)=\alpha \\ g(r=R_1)=\alpha \end{cases}. \tag{4.8}$$

Finally, introducing equations 4.7 inside 4.1 and 4.2 and taking into account 4.8, solutions for $f(r)$ and $g(r)$ can be found so that we already know field profiles inside the material

$$f(r)=\mu_r\mu_\phi\left(\frac{r}{R_2}\right)^{-1+\mu_\phi} \implies H_r^{mid}(r)=H_a\mu_\phi\left(\frac{r}{R_2}\right)^{-1+\mu_\phi} sin\phi, \tag{4.9}$$

$$g(r)=\left(\frac{r}{R_2}\right)^{-1+\mu_\phi} \implies H_\phi^{mid}(r)=H_a\left(\frac{r}{R_2}\right)^{-1+\mu_\phi} cos\phi. \tag{4.10}$$

Notice that we solve two first-order differential equations, so that only two constants have to be determined. However solutions must fulfill the four boundary conditions. This fact leads to obtain two extra constrains

$$\mu_r\cdot\mu_\phi=1, \tag{4.11}$$

$$\alpha=\left(\frac{R_1}{R_2}\right)^{\mu_\phi-1}. \tag{4.12}$$

The first one imposes that both permeabilities must be inverse to each other. The second one relates the inner field scale factor α with radius R_1 and R_2 and the angular (or the radial, due to equation 4.11) permeability.

From equation 4.12 we can see that the α factor (i.e. magnetic field inside the device) decreases as angular permeability increases because $R_1/R_2<1$. This happens because magnetic field becomes concentrated near the outer radius R_2 (from expressions 4.9 and 4.10). And that's why such homogeneous anisotropic device can be used to achieve an approximate cloaking: we can choose a couple of inverse permeabilities such that they make the inner field arbitrary small. As this field can be reduced as much as need, the interaction with magnetic objects placed inside can also be arbitrary minimized so that we can obtain a good cloaking behavior only setting suitable permeabilities of the shell. Interestingly, it can be demonstrated that null distortion is also obtained for *any* non-uniformly applied magnetic field.

For example, for the case $R_1=0.1m$, $R_2=0.2m$ and $\mu_\phi=6$ ($\mu_r=1/6\approx0.167$) the field inside becomes scaled by a $\alpha\approx0.03125$. If $\mu_\phi=10$ ($\mu_r=0.1$) then $\alpha\approx0.00195$. Both two cases have been numerically simulated to check corresponding inner field scaling factors. From this simulations we can also see how magnetic field lines are expelled from the inner region (see figure 4.2).

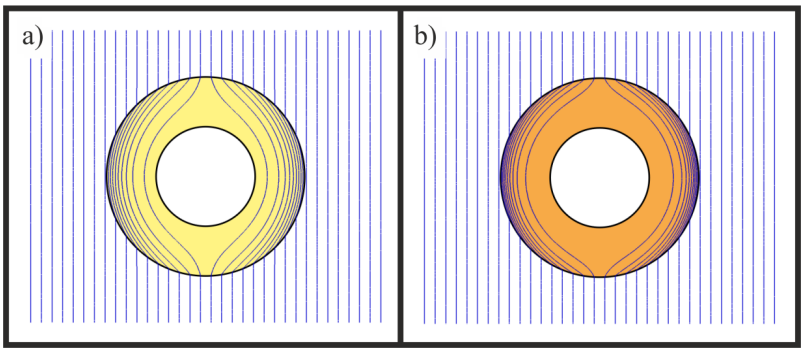

Figure 4.2: Field lines interacting with two homogeneous anisotropic devices. In the first one (a) $\mu_\phi=6$, $\mu_r=1/6$ and in the second one (b) $\mu_\phi=10$, $\mu_r=1/10$. We clearly see that increasing the angular permeability causes magnetic fields to concentrate near the outer radius.

In spite of achieving magnetic cloaking, these homogeneous cloaks are not antimagnets, because the magnetic field created by a source in its interior will leak to the exterior. To avoid this, we can make us of a superconducting layer placed at the inner surface of the cloak, as discussed in section 4.1. Introducing

such a layer does not substantially modify the property of cloaking, as long as μ_ϕ is sufficiently larger than 1, because in this case the magnetic field coming from external sources will be almost excluded from the central region and the interaction with the superconducting layer will be negligible. In this way an antimagnet design is being outlined: an inner superconducting layer and an outer homogeneous shell. However, this scheme alone cannot yet solve our goal of a feasible antimagnet, because the material in the outer shell, even though it would have a constant permeability, would require fine-tuned anisotropic values ($\mu_\phi = 1/\mu_r$). Such materials are not available.

4.3 Antimagnet design: discretization of the angular and radial components with two types of feasible layers

In this section we will transform the homogeneous cloak with uniform and anisotropic parameters described in previous section into one made with realistic materials. To do this one could propose a device in which there were only two types of layers: one of them only provides the angular component of permeability and the other one only provides the radial. By alternating those kind of layers and tuning their parameters an effective homogeneous anisotropic behavior could be achieved. However, this idea is still too demanding, because we would need two type of anisotropic layers: layers that provide the angular component (we call them *A-type* layers) must have high tangential tunable permitivity ($\mu_\phi^A > 4$ as we already discussed in the previous section) and radial permitivity equal to one ($\mu_r^A = 1$). On the other hand layers providing the radial component (we call them *R-type* layers) must have small radial tunable permitivity ($\mu_r^R < 0.25$) and angular permitivity equal one ($\mu_\phi^R = 1$). In fact these *R-type* layers could be realized with metamaterial-like materials made of arrays of superconducting plates (the precise radial permeability tunable by changing the distances between plates) [59, 60]. Nevertheless there exist no any material that satisfies the anisotropy needed to build *A-type* layers, with such high values of angular permeability.

In spite of this type of discretization we propose another strategy: we substitute these anisotropic *A-type* layers by isotropic layers with a suitable permitivity $\mu^A = \mu_r^A = \mu_\phi^A$. These layers would give the necessary angular permitivity but they would also contribute with an undesired radial permitivity. However, this could be counteracted by tuning the radial permitivity of the *R-type* layers to smaller values. The main advantage of this configuration is that both type of layers are in principle already available. One of them built with arrays of superconducting plates and the other one made of non-hysteretic superparamagnetic materials (i.e. ferromagnetic nanoparticles embedded in a non-magnetic media [61]). In the next section we will explain the tuning process by which μ_r^R and μ^A can be determined in order to minimize the field distortion caused by the antimagnet.

4.3.1 Tuning process

There are three relevant parameters that must be taken into account in the tuning process: μ_r^R, μ^A and the total number of layers. We start fixing a total number of layers (an even number, as we want as many *A-type* layers as *R-type*) and a permitivity for the *A-type* layers (always placing an ideal superconducting layer in the inner surface, as we discussed in section 4.1). Then the μ_r^R parameter is tuned following a numerical iterative method in order to minimize the distortion appeared outside the device (for a given applied field).

A first case with 10 layers (5 *A-type* layers, 5 *R-type* plus the inner superconducting one that we don't count) is presented. The outer layer is a *A-type* and we fix a permeability for these layers $\mu^A = 6$ (we choose this value because the corresponding homogeneous anisotropic cloak discussed in section 4.2 leads to an $\alpha \approx 0.03125$, so that magnetic field entering inside R_1 is almost negligible). We apply an external uniform magnetic field ($\mathbf{H}_a = H_a \hat{\mathbf{u}}_y$) and then we evaluate the distortion appeared outside depending on the radial permitivity of the *R-type* layers. We choose an starting value for $\mu_r^R = 1/6 \approx 0.167$, knowing that the optimized value will be, in general, smaller than this because of the additional radial permitivity added by the isotropic *A-type* layers. To evaluate the distortion appeared we perform a

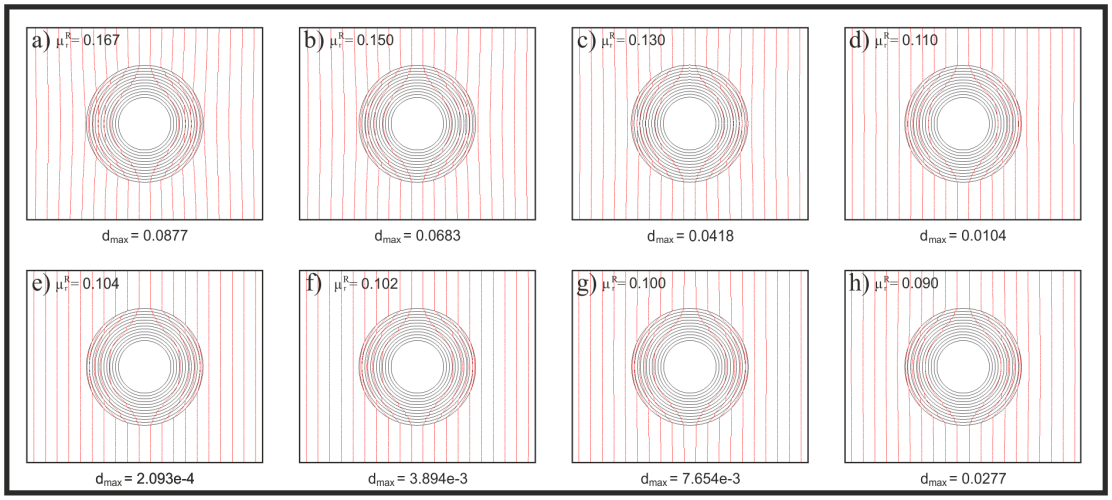

Figure 4.3: Field lines for different values of μ_r^R (and $\mu_r^A = 6$). It can be clearly seen that above the optimized value there is too much "ferromagnetic" contribution that tends to concentrate field lines inside the device. On the other hand, below the optimized value *R-type* layers "diamagnetic" contribution dominates so that magnetic field is expelled. This clear trend that can be easily quantized through the d_{max} parameter lets us rapidly find the optimal μ_r^R value for a uniform applied field.

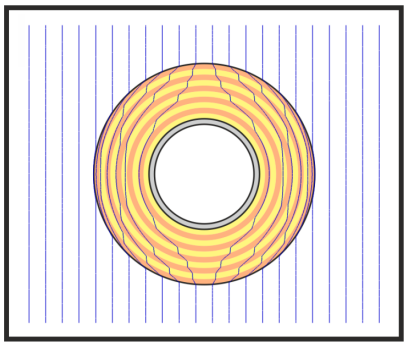

Figure 4.4: Simulation of the final antimagnet design with 10 layers interacting with a uniform applied field. *A-type* layers are painted orange ($\mu_r^A = \mu_\phi^A = \mu^A = 6$) and *R-type* layers are painted yellow ($\mu_r^R = 0.104$, $\mu_\phi^R = 1$). The inner grey layer represents an ideal superconductor in Meissner state with negligible penetration depth ($\mu = 0$).

COMSOL simulation for each μ_r^R value. Then we define a *distortion function* $d(\mathbf{r})$ as

$$d = \left(\frac{(B_x - B_{x,a})^2 + (B_y - B_{y,a})^2}{B_{x,a}^2 + B_{y,a}^2} \right)^{\frac{1}{2}}, \tag{4.13}$$

where B_x and B_y are the two components of the total field and $B_{x,a}$ and $B_{y,a}$ are the components of the applied field. This function represents the ratio of distortion appeared in each point of exterior space respect to the applied field. In each COMSOL simulation we compute this function along the exterior space and we take the maximum value (this maximum distortion is always found in points near the outer radius R_2) as a comparing criteria. Some captions about this iterative process are shown in figure4.3. Following the process we see that field lines distortion (they should be perfectly vertical) reduces as μ_r^R descreases. In particular, in the first cases (a-f) field lines tend to "enter" inside the device (there is a more intense ferromagnetic contribution given by the *A-type* layers that dominates front the diamagnetic contribution given by the *R-type* layers). Distortion minimizes in figure 4.3e, where field lines look vertical and d_{max} is minimized. If we go on decreasing μ_r^R (f-h) then the diamagnetic contribution dominates and there appears distortion in the opposite direction: field lines tend to be expelled from the device. This clear trend lets one to easily find the value that minimizes distortion for a certain antimagnet configuration. In this case we conclude that uniform applied field distortion minimizes choosing: $\mu_r^A = 6$ and $\mu_r^R = 0.104$ (figure 4.4).

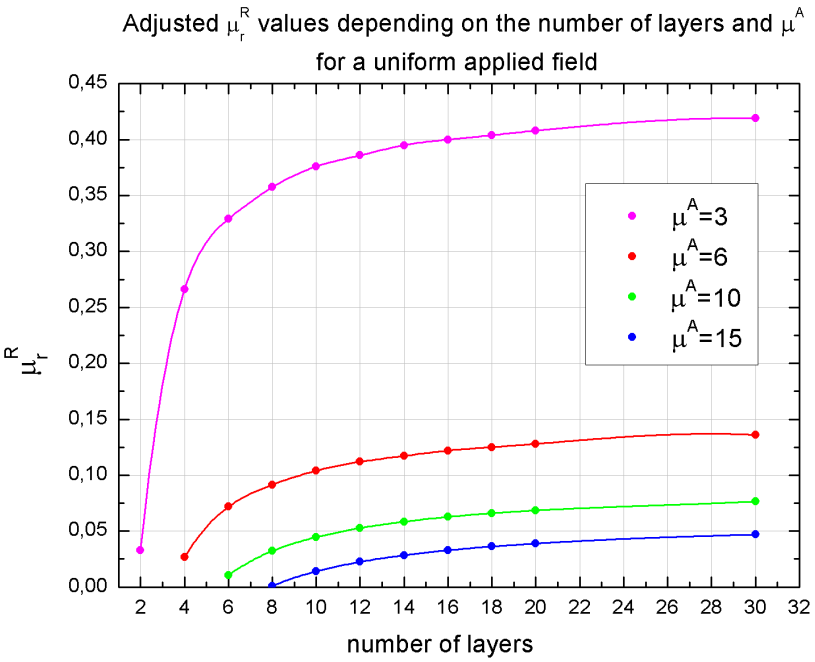

Figure 4.5: Tuned μ_r^R values depending on the number of layers and the permitivity of the *A-type* layers. Comparing any two of the plotted series we notice that, except the first two points, there is a constant shift between the adjusted values. It is also interesting to see that adjusted permeabilities seem to saturate for high number of layers.

4.3.2 Tuning process for other configurations

In the previous section 4.3.1 we explained there are three relevant parameters: μ_r^R, μ^A and the total number of layers. We decided to study a first case fixing a 10 layers configuration and $\mu^A = 6$.

However the tuning process we have explained can be applied in other cases with different number of layers, for example. This leads to obtain a curve that indicates adjusted μ_r^R for each case. At the same time we can repeat this process for other values of μ^A. As we already explained taking higher values will tend magnetic fields to concentrate near the outer radius while lower values will let field go inside. This second case could be problematic because if *A-type* layers permeability is decreased enough intense magnetic will try to penetrate inside R_1. This does not finally happen as a superconducting layer is placed in the inner surface but it could cause distortion outside. However, similar μ_r^R tuning process shows that the total distortion for a uniform applied field can be canceled even in these cases. Final adjusted μ_r^R curves for different numbers of layers and several μ^A choices is shown in figure 4.5.

From this plot some interesting conclusions can be extracted. First of all we can see how all lines (for a fixed μ^A) tend to saturate for a high numbers of layers and each one converges to a certain value of μ_r^R . A second relevant conclusion is that given any two series the difference between the adjusted μ_r^R for any number of layers (except the first two cases with less layers) keeps a constant value.

4.3.3 Evaluation of the antimagnet behavior depending on its specific characteristics

In the previous two sections we have explained the tuning process always assuming a uniform applied field. Now it is necessary to check how these antimangets behave when other kind of fields are applied. We have chosen two representative fields to do this evaluation: field created by a current wire and field created by a magnetic dipole (equivalent to the field created by a small permanent magnet). While uniform applied field has no spatial variation, current wire field and dipolar field do change depending on the precise spatial point. This lets us study whether the applied field inhomogeneity is related with the distortion caused by a certain antimagnet. The first interesting conclusion is that in these cases with non-uniform applied field antimagnets do cause distortion of exterior field (different from what happened

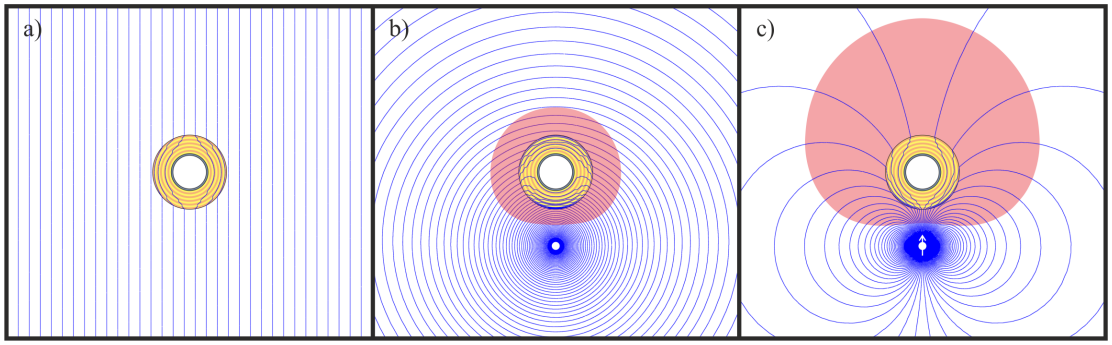

Figure 4.6: 10 layers antimagnet with $\mu^A = 6$ and $\mu_r^R = 0.104$ interacts with different applied fields. In figure a, a uniform field is applied, in b we apply a current wire field and in c a dipolar field (wire and dipole are placed at a distance of 0.4 meters of the antimagnet center). Regions shaded pink indicate places where distortion is larger than 0.01.

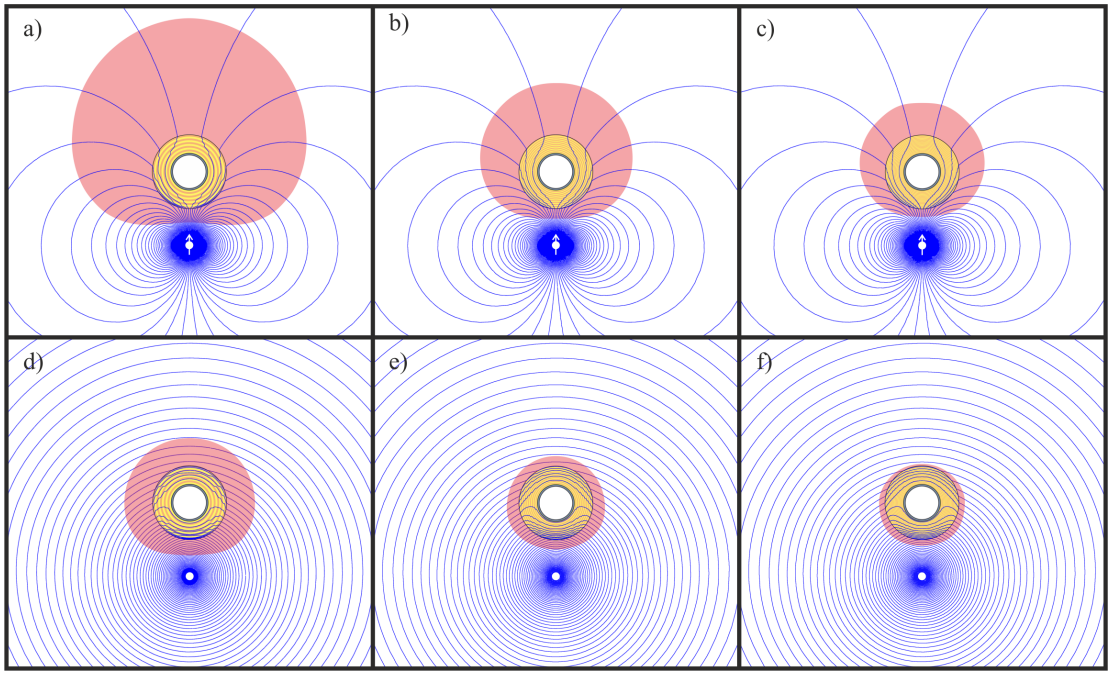

Figure 4.7: Antimagnets with 10, 20 and 30 layers (plus a inner superconducting isotropic layer) interact with dipolar field (a-c) and current wire field (d-f). Pink-shaded regions where $d > 0.01$ show an improvement of the antimagnet behavior when the number of layers is increased for both non-uniform applied fields.

when a uniform field was applied and distortion function d reached negligible values). To quantitatively evaluate this distortion we have computed distortion function d (defined in expression 4.13) outside the device and we have shaded pink regions where $d > 0.01$. Results are shown in figure 4.6.

From these simulations a clear conclusion can be extracted: the higher inhomogeneous applied field is, the higher distortion a certain antimagnet causes. Nevertheless it is worth to explore behavior of other antimagnet configurations with higher number of layers when these inhomogeneous fields are applied. In figure 4.7 we present simulations of antimagnets with $\mu^A = 6$ and 10, 20 and 30 layers (for which adjusted μ_r^R values can be found in plot 4.5 and are 0.104, 0.128 and 0.136 respectively) interacting with dipolar and current wire fields.

In these cases results are really clarifying, showing that antimagnets with higher number of layers tend to reduce distortion of any inhomogeneous applied field. This is evident for the dipolar field case (figures a-c) and similar trend is shown for the current wire field (figures d-f). It is not difficult to justify this behavior, because configurations with higher number of layers constitute a more accurate discretization of the homogeneous anisotropic cases (explained in section 4.2), which we already said that caused no exterior field distortion for any applied field.

Finally, we need to know if the distortion regions showed in figures 4.6 and 4.7 are "large" or not in order to know if our design achieves significant distortion reduction. As we explained in section 3.2.3 distortion caused by a magnetic material naturally decreases so that they always become undetectable if observer goes far enough. That's why we have compared these distortion regions with the ones created by some reference materials that we have chosen to be a perfect superconducting shell and an infinite-permeability ferromagnetic shell (with same sizes R_1 and R_2). In these cases distortion regions in which $d > 0.01$ extend much farther than the limits shown in captions. This means that proposed antimagnets do get a substantial reduction of the exterior field distortion even when non-homogeneous fields are applied compared with materials that also enable magnetic shielding.

This study has been done using antimagnet designs with all $\mu^A = 6$ (red points in figure 4.5). Same behavior is found when we repeat this study with other configurations with higher permeabilities for the *A-type* layers. However these cases need *R-type* layers to have very low radial permeabilities μ_r^R. This leads to practical problems, as it is reported in reference [60] because it would imply that the superconducting layers forming these *R-type* layers should be put very close one from another. On the other hand antimagnets with low permeabilities for the *A-type* layers exhibit similar behavior, and for a small number of layers they cause smaller distortion than configurations with higher μ^A with the same number of layers. However these cases differentiate because increasing the number of layers leads to an improvement (decrease of field distortion) that rapidly saturates, meaning that the distortion region is not reduced when we increase over a certain number of layers. Simulations done with previous dipolar field have shown that antimagnets with $\mu^A = 3$ with 20 and 30 layers create almost the same distortion region.

For all these reasons most of this chapter has been dedicated to antimagnet configurations with intermediate μ^A values, which are the best candidates for a future hypothetical practical implementation.

4.4 Limitations of the proposed antimagnet designs

Devices proposed in this chapter have been developed and tuned assuming certain idealizations. This has been done in order to simplify the design task. However a more realistic approach would be need to discuss the realistic possibilities of these designs. In this section we enumerate the most relevant assumptions that we have done and we briefly discuss how they limit or not the viability of these devices.

- **All superconductors are assumed to be in Meissner state (and doing a *complete exclussion* of the magnetic field, so that penetration dept is 0)**: This assumption affects two parts of the antimagnet designs: the inner homogeneous superconducting layer and the *R-type* layers. Any realistic application would need magnetic fields larger than the lower critical field H_{c1} for type-II superconductors (or the H_c for type-I) so that magnetic field would not be completely expelled by the superconductors and it would penetrate inside them. Concerning the inner layer this could be solved using a type-II superconductor (like most high-temperature ones) with a high critical-current density. In these cases the strong pinning causes that magnetic field only penetrates a small thickness inside the material, so that currents circulate mainly in a thin layer in the surface giving a response very similar to the Meissner one with almost null penetration dept [62]. Implications related with the *R-type* layers are also solvable. Field penetration inside the superconducting layers would make its diamagnetic response weaker (so μ_r^R would be nearer to 1). However this could be solved retuning permeability of the *A-type* layers so that the final system would not cause distortion of a uniformly applied magnetic field.

- ***A-type* layers are assumed to be non-hysteretic**: In our explanation we assume that *A-type* layers give a fixed paramagnetic response independent of the external applied field and of its magnetic history. However, any practical application would imply a variation of magnetic field, so that these layers had to have a constant response. As we already pointed, this could be achieved not using a simple paramagnetic material but a superparamagnetic one (or a composite of superparamagnetic nanoparticles embedded in a non-magnetic matrix). These materials exhibit almost no magnetic hysteresis (for a certain range of applied magnetic fields) so that they give an approximate constant response.

- **Fine tunability of layers permeability is assumed**: We have explained how *R-type* layers have to be tuned (for a certain μ^A) in order to minimize distortion of a uniformly applied magnetic field. We have given permeabilities with 4 significant digits, which requires an extremely fine tuning. From a practical point of view this cannot be achieved and real values would fluctuate between a certain interval. This means that hypothetical real antimagnets would cause certain field distortion even for a uniform applied field. Although it has not been deeply studied this could be minimized choosing configurations with a higher number of layers, because in these cases it seems that there exists a certain tolerance between the optimum values so that fluctuations do not lead to high external field distortions. In any case, the effect on the performance of an antimagnet because some tolerance on their constitutive values could be theoretically studied with our approach.

Chapter 5

Conclusions

Along the previous chapters we have studied several electromagnetic devices and phenomena that have let us finally conclude with a technique to design feasible magnetostatic cloaking devices (that we have called *antimagnets*). However, apart from these final designs, some other significant conclusions have been extracted. In the following points we try to summarize all relevant conclusions that we have found and studied in this project.

- Electromagnetic *cloaking* concept that allows invisibility can be extended to the magnetostatic regime. In static conditions the detection of a magnetic material can be done due to the fact that, in general, these materials distort an external applied magnetic field. This distortion can be detected by the magnetic source (that feels a force or a torque) or by any other detector, revealing the presence of the object. Because of this a magnetic cloaking must be a device such that deviates magnetic fields avoiding an inner region (which will contain the magnetic object we want to hide) and, at the same time, it does not have to cause distortion of the externally applied magnetic field. If these conditions are fulfilled, neither the magnetic object placed inside the device nor the magnetostatic cloak itself will be magnetically detectable, achieving total magnetostatic "invisibility".

- Transformation optics technique used to design electromagnetic metamaterials can also be applied in order to tailor a magnetic material that allows an specific control of static magnetic fields. However, cases that involves spatial topological changes (like in the typical cloaking case in which a "punctual expansion" is done) have to be carefully discussed and material parameters obtained in these cases must be rechecked starting from basic Maxwell's equations (if we want to check the validity in the magnetostatics regime we must do so using the reduced set of magnetostatic Maxwell's equations).

- There exist several ways to achieve magnetostatic cloaking. Permitivities obtained from transformation optics technique doing a linear space transformation allow exact magnetostatic cloaking. However there exist simpler material parameters that enables approximate magnetostatic cloaking. In particular we have mathematically seen that an homogeneous anisotropic shell with inverse permeabilities causes zero distortion of any external applied field and it also lets to arbitrarily reduce magnetic field that penetrates inside it (increasing the angular permeability leads to an arbitrary reduction of the magnetic field inside). Penetration of the external magnetic field can be avoided if an *ideal superconducting shell is placed at the inner radius* R_1. This shell does not cause substantial field distortion as long as angular permeability is large enough, because in this case only weak magnetic fields reach the superconductor in the inner surface. At the same time this layer ensures that field created by any magnetic source placed inside the superconductor does not leak to the exterior.

- It is possible to do a discretization of this homogeneous anisotropic shell in a series of feasible alternating layers of two types. One kind of layers (*A-type*) are homogeneous and isotropic with permeabilities larger than 1. They can be built with superparamagnetic materials (in order to have no hysteresis). The second type of layers (*R-type*) are metamaterial-like because we need they are

homogeneous but anisotropic. They have to have angular permeability equal 1 and tunable radial permeability between 0 and 1. These layers can be built using arrays of superconducting plates. Fixing a certain permitivity value for the *A-type* layers and placing the ideal superconducting shell inside a tuning process leads to find the radial permeability of *R-type* layers that minimizes distortion of a uniformly applied magnetic field. That is the way by which we can design a certain *antimagnet*, for a given number of layers and a fixed permeability for the *A-type* layers.

- For a uniformly applied magnetic field distortion caused by each antimagnet design is basically negligible. However, when non-uniform fields are applied antimagnets do cause exterior field distortion. This distortion has been evaluated by plotting regions where a distortion function d is larger than 0.01. We have seen that distortion caused by a certain antimagnet increases as the applied field is more inhomogeneous (see comparisons between the current wire field and the dipolar field). At the same time we have checked that distortion appeared by a certain non-homogeneous applied field is reduced as long as we use antimagnets with larger number of layers.

- Although designs proposed in this project still present important fabrication difficulties and they have non-negligible limitations we think they represent a relevant step towards a future realistic implementation of invisibility ideas applied to the magnetostatic regime. We think there are several fields in which such devices could suppose important advantages, for example in helping patients with iron-containing implants to access to magnetic resonance tests or in reducing the magnetic signature of vessels and planes.

Appendix A

Validity of the electromagnetic cloaking parameters to obtain magnetostatic cloaking

In this section we will check that material parameters obtained by transformation optics (doing a linear compression, as it is explained in section 2.3.1) that make electromagnetic cloaking also enable cloaking of static magnetic fields. We start with material parameters expressed in equations 2.12-2.14. Of course we only take care of permeabilities because we are interested in the magnetostatic regime. Due to the translational symmetry along the z axis, fields cannot have components in this direction so that permeability component $\mu_{z'z'}$ does not play any role. Then we only deal with the following permeabilities

$$\mu_{rr}(r) = \frac{r - R_1}{r}, \tag{A.1}$$

$$\mu_{\phi\phi}(r) = \frac{r}{r - R_1}. \tag{A.2}$$

Given a uniformly applied magnetic field in the y direction (following the notation expressed in figure 4.1) these permeabilities must fulfill magnetostatic Maxwell's equations. At the same time we impose a uniformly applied magnetic field outside (what guarantees that there is no distortion outside the material) and zero field inside the inner radius

$$\mathbf{H}^{out} = \mathbf{H}_a, \tag{A.3}$$

$$\mathbf{H}^{in} = 0. \tag{A.4}$$

Of course magnetostatic Maxwell's equations 3.1, 3.2 must be fulfilled everywhere, in particular inside the material. There, induction and magnetic field components are related through the permeabilities as: $\mathbf{B}_r^{mid} = \mu_0\mu_r\mathbf{H}_r^{mid}$ and $\mathbf{B}_\phi^{mid} = \mu_0\mu_\phi\mathbf{H}_\phi^{mid}$. Using the translational symmetry along the z axis and the fact that there are no free currents nor free charges inside the material these Maxwell's equations become

$$\frac{1}{r}H_r^{mid} + \frac{r - R_1}{r}\frac{\partial H_r^{mid}}{\partial r} + \frac{1}{r - R_1}\frac{\partial H_\phi^{mid}}{\partial \phi} = 0, \tag{A.5}$$

$$H_\phi^{mid} + r\frac{\partial H_\phi^{mid}}{\partial r} - \frac{\partial H_r^{mid}}{\partial \phi} = 0, \tag{A.6}$$

where we have already used permeability expressions A.1 and A.2. Equations A.3 and A.4 can be rewritten as

$$\begin{cases} H_r^{out} = H_a sin\phi \\ H_\phi^{out} = H_a cos\phi \end{cases}, \qquad \begin{cases} H_r^{in} = 0 \\ H_\phi^{in} = 0 \end{cases}. \tag{A.7}$$

And boundary conditions (continuity of the normal component of $\mathbf{B}$ and the tangential component of $\mathbf{H}$ at the interfaces $r = R_1$ and $r = R_2$) impose

$$\begin{cases} H_r^{mid}(r = R_2) = \frac{R_2}{R_2 - R_1} H_a sin\phi \\ H_\phi^{mid}(r = R_2) = H_a cos\phi \end{cases}, \qquad \begin{cases} H_r^{mid}(r = R_1) = 0 \\ H_\phi^{mid}(r = R_1) = 0 \end{cases}. \tag{A.8}$$

To solve equations A.5 and A.6 with boundary conditions expressed in A.8 we make the same type of guess we did in section 4.2 and we suppose that solutions can be written as a product of the angular and the radial part

$$\begin{cases} H_r^{mid}(r) = f(r) \frac{R_2}{R_2 - R_1} H_a sin\phi \\ H_\phi^{mid}(r) = g(r) H_a cos\phi \end{cases}, \tag{A.9}$$

where $f(r)$ and $g(r)$ are arbitrary radially-dependent functions that must be found. Doing so boundary conditions expressed in A.8 become

$$\begin{cases} f(r = R_2) = 1 \\ g(r = R_2) = 1 \end{cases}, \qquad \begin{cases} f(r = R_1) = 0 \\ g(r = R_1) = 0 \end{cases}. \tag{A.10}$$

Defining $\gamma = R_2/(R_2 - R_1)$ and taking into account A.9 Maxwell's equations A.5 and A.6 become

$$(r - R_1)\gamma f(r) + (r - R_1)^2 \gamma f'(r) - r g(r) = 0, \tag{A.11}$$

$$g(r) + r g'(r) - \gamma f(r) = 0, \tag{A.12}$$

which are two first-order differential equations (primes indicate derivatives respect r), whose solutions will have 2 constants to be determined by the boundary conditions. To solve this we combine these equations in one second-order differential equation. Isolating $g(r)$ from A.11

$$g(r) = \gamma \frac{r - R_1}{r} f(r) + \gamma \frac{(r - R_1)^2}{r} f'(r), \tag{A.13}$$

$$g'(r) = \gamma \frac{R_1}{r^2} f(r) + \gamma \frac{2r^2 - R_1^2 - rR_1}{r^2} f'(r) + \gamma \frac{(r - R_1)^2}{r} f''(r), \tag{A.14}$$

and substituting $g(r)$ and its derivative in A.12 we get

$$3f'(r) - (R_1 - r) f''(r) = 0. \tag{A.15}$$

The general solution of this differential equation is expressed in equation A.16. On the other hand, f is related with g through equation A.13 so that

$$f(r) = -\frac{C_1}{2(r - R_1)^2} + C_2, \tag{A.16}$$

$$g(r) = \gamma \frac{C_1}{2r(r - R_1)} + \gamma \frac{C_2 (r - R_1)}{r}. \tag{A.17}$$

Now we have to determine constants imposing the 4 boundary conditions expressed in A.8. Although solutions only have two free constants (C_1 and C_2), *solution must fulfill the four equations* to ensure that permeabilities expressed in equations A.1 and A.2 enable the desired cloaking behavior. Actually that is what happens if $C_1 = 0$ and $C_2 = 1$, so that f and g functions are

$$f(r) = 1, \tag{A.18}$$

$$g(r) = \gamma \frac{r - R_1}{r}, \tag{A.19}$$

and fields inside the material are

$$\begin{cases} H_r^{mid} = \frac{R_2}{R_2 - R_1} H_a sin\phi \\ H_\phi^{mid} = \frac{R_2}{R_2 - R_1} \left(1 - \frac{R_1}{r}\right) H_a cos\phi \end{cases}, \qquad \begin{cases} B_r^{mid} = \mu_0 \frac{r - R_1}{r} \frac{R_2}{R_2 - R_1} H_a sin\phi \\ B_\phi^{mid} = \mu_0 \frac{r}{r - R_1} \frac{R_2}{R_2 - R_1} \left(1 - \frac{R_1}{r}\right) H_a cos\phi \end{cases}, \tag{A.20}$$

what proves that permeabilities expressed in equations A.1 and A.2 obtained applying transformation optics technique also enable magnetostatic cloaking. To guarantee that this result is completely valid we can repeat the last part of the development isolating $f(r)$ from A.12 and substituting it and its derivative in equation A.11. The differential equation that we get is

$$-R_1 g'(r) + (3r^2 - 5rR_1 + 2R_1^2)g'(r) + (r - R_1)^2 r g''(r) = 0. \tag{A.21}$$

In this case the general solution of this differential equation is

$$g(r) = \frac{2C_1 + r(r - 2R_1)C_2}{2r(r - R_1)}. \tag{A.22}$$

Imposing boundary conditions (A.10) for g we determine constants and it becomes

$$g(r) = \frac{R_2}{R_2 - R_1}\frac{r - R_1}{r}. \tag{A.23}$$

And using the relation between f and g obtained isolating f in A.12 we find

$$f(r) = 1, \tag{A.24}$$

which are the same solutions as the ones obtained previously in the first part of the development.

Bibliography

[1] J. C. Quintana and F. L. Aguilar, *Interacción Electromagnética. Teoría clásica*. Barcelona, España: Reverté, (2007).

[2] U. Leonhardt and T. Philbin, *Geometry and Light. The Science of Invisibility*. Mineola, New York: Dover Publications , Inc., (2010).

[3] W. Weiglhofer and A. Lakhtakia, *Introduction to complex mediums for optics and electromagnetics*. Bellingham, WA, USA: SPIE Press, (2003).

[4] T. J. Cui, D. R. Smith, and R. Liu, *Metamaterials*. New York, USA: Springer, (2010).

[5] C. Caloz and T. Itoh, *Electromagnetic Matematerials, Transmission Line Theory and Microwave Applications*. Hoboken, New Jersey, USA: Wiley, (2006).

[6] D. R. Smith, J. Pendry, and M. C. K. Wiltshire, "Metamaterials and negative refractive index," *Science*, vol. 305, p. 788, (2004).

[7] V. Veselago, "The electrodynamics of substances with simultaneously negative values of μ and ε," *Sov. Phys. Usp.*, vol. 10, p. 509, (1968).

[8] L. Mandlshtam, "Zhurnal eksperimentalnoii teoreticheskoi fiziki," *Zhurnal Technicheskoi Fiziki*, vol. 15, pp. 476–478, (1945).

[9] G. Malyuzhinets, "A note on the radiation principle," *Zhurnal Technicheskoi Fiziki*, vol. 21, pp. 940–942, (1951).

[10] D. Sivukhin, "The energy of electromagnetic waves in dispersive media," *Opt. Spektrosk*, vol. 3, pp. 308–312, (1957).

[11] R. Hutter, "Beam and wave electronics in microwave tubes," *Van Nostrand Reinhold, Princeton, NJ*, pp. 220–230, (1960).

[12] J. Altman, "Microwave circuits," *Van Nostrand Reinhold*, p. 304, (1964).

[13] R. Silin and V. Sazonov, "Slow-wave structures," *Moscow, Soviet Radio*, (1966).

[14] R. Silin, "Waveguiding properties of two-dimensional periodical slow-wave systems," *Voprosy Radioelektroniki. Elektronika*, vol. 4, pp. 11–33, (1959).

[15] E. Hecht, *Optics (4th Edition)*. Addison Wesley, 4 ed., Aug. (2001).

[16] J. Pendry, A. Holden, W. Stewart, and I. Youngs, "Extremely low frequency plasmons in metallic mesostructures," *Phys. Rev. Lett.*, vol. 76, pp. 4773–4776, (1996).

[17] J. Pendry, A. Holden, D. Robbins, and W. Stewart, "Magnetism from conductors and enhanced nonlinear phenomena," *IEEE Trans. Micro. Theory Tech.*, vol. 47, pp. 2075–2084, (1999).

[18] D. R. Smith, W. J. Padilla, D. C. Vier, S. C. Neumat-Nasser, and S. Schultz, "Composite medium with simultaneously negative permeability and permittivity," *Phys. Rev. Lett.*, vol. 84, p. 4184, (2000).

[19] R. A. Shelby, D. R. Smith, and S. Schultz, "Experimental verification of a negative index of refraction," *Science*, vol. 292, pp. 77–79, (2001).

[20] J. Pendry, "Negative refraction makes a perfect lens," *Phys. Rev. Lett.*, vol. 85, p. 3966, (2000).

[21] D. Smith, D. Schurig, M. Rosenbluth, S. Schultz, S. Ramakrishna, and J. Pendry, "Limitations on subdiffraction imaging with a negative refractive index slab," *Appl. Phys. Lett.*, vol. 82, p. 1506, (2003).

[22] J. Baena, R. Marques, F. Medina, and J. Martel, "Artificial magnetic metamaterial design by using spiral resonators," *Phys. Rev. B*, vol. 69, p. 014402, (2004).

[23] J. Huangfu, L. Ran, H. Chen, X. Zhang, K. Chen, Grzegorczyk, and J. T.M., Kong, "Experimental confirmation of negative refractive index of a metamaterial composed of omega-like metallic patterns," *Appl. Phys. Lett.*, vol. 84, pp. 1537–1539, (2004).

[24] T. Cui and J. Kong, "Time-domain electromagnetic energy in a frequency-dispersive lefthanded medium," *Phys. Rev. B*, vol. 70, p. 205106, (2004).

[25] T. Cui, Q. Cheng, W. Lu, Q. Jiang, and J. Kong, "Localization of electromagnetic energy using a left-handed medium slab," *Phys. Rev. B*, vol. 71, p. 045114, (2005).

[26] T. Taubner, D. Korobkin, Y. Urzhumov, and et al., "Near-field microscopy through a sic superlens," *Science*, vol. 313, pp. 1595–1595, (2006).

[27] A. Iyer and G. Eleftheriades, "Negative refractive index metamaterials supporting 2-d waves," *IEEE-MTT-S*, vol. 2, pp. 412–415, (2002).

[28] A. Oliner, "A periodic-structure negative-refractive-index medium without resonant elements," *IEEE-AP-S Digest*, p. 41, (2002).

[29] C. Caloz and T. Itoh, "Application of the transmission line theory of left-handed (lh) materials to the realization of a microstrip lh transmission line," *IEEE-AP-S Digest*, vol. 2, pp. 412–415, (2002).

[30] A. Iyer, P. Kremer, and G. Eleftheriades, "Experimental and theoretical verification of focusing in a large, periodically loaded transmission line negative refractive index metamaterial," *Opt. Express*, vol. 11, pp. 696–708, (2003).

[31] C. Caloz and T. Itoh, "Transmission line approach of left-handed (lh) structures and microstrip realization of a low-loss broadband lh filter," *IEEE Trans. Antennas Propagat.*, vol. 52, pp. 1159–1166, (2004).

[32] D. Smith, J. Mock, A. Starr, and D. Schurig, "Gradient index metamaterials," *Phys. Rev. E*, vol. 71, p. 036609, (2005).

[33] U. Leonhardt, "Optical conformal mapping," *Science*, vol. 312, pp. 1777–1780, (2006).

[34] J. Pendry, D. Schurig, and D. Smith, "Controlling electromagnetic fields," *Science*, vol. 312, pp. 1780–1782, (2006).

[35] R. Liu, C. Ji, J. Mock, J. Chin, T. Cui, and D. Smith, "Broadband ground-plane cloak," *Science*, vol. 323, p. 366, (2009).

[36] D. Schurig, J. Mock, B. Justice, and et al., "Metamaterial electromagnetic cloak at microwave frequencies," *Science*, vol. 314, pp. 977–980, (2006).

[37] M. Rahm, D. Schuring, D. A. Roberts, S. A. Cummer, D. R. Smith, and J. B. Pendry, "Design of electromagnetic cloaks and concentrators using form-invariant coordinate transformations of maxwell's equations," *Photonics and Nanostructures*, vol. 6, pp. 87–95, (2008).

[38] S. Cummer, P. Bogdan-Ioan, D. Schurig, and D. Smith, "Full-wave simulations of electromagnetic cloaking structures," *Phys. Rev. E.*, vol. 74, p. 036621, (2006).

[39] J. B. Pendry, "Metamaterials and the control of electromagnetic fields," *Proceedings of the Ninth Rochester Conference on Coherence and Quantum Optics*, (2007).

[40] W. X. Jiang, T. J. Cui, X. M. Yang, Q. Cheng, R. Liu, and D. R. Smith, "Invisibility cloak without singularity," *Appl. Phys. Lett.*, vol. 93, no. 19, p. 194102, (2008).

[41] T. Han, X. Tang, and F. Xiao, "Ellipsoidal cloak for inhomogeneous medium," in *Microwave and Millimeter Wave Technology (ICMMT), 2010 International Conference on*, pp. 1665 –1668, may (2010).

[42] W. Yan, M. Yan, Z. Ruan, and M. Qiu, "Coordinate transformations make perfect invisibility cloaks with arbitrary shape," *New Journal of Physics*, vol. 10, no. 4, p. 043040, (2008).

[43] J. Hu, X. Zhou, and G. Hu, "Design method for electromagnetic cloak with arbitrary shapes based on laplace's equation," *Opt. Express*, vol. 17, pp. 1308–1320, Feb (2009).

[44] W. Jiang, T. Cui, Q. Cheng, J. Chin, X. Yang, R. Liu, and D. Smith, "Design of arbitrarily shaped concentrators based on conformally optical transformation of nonuniform rational b-spline surfaces," *Appl. Phys. Lett.*, vol. 92, p. 264101, (2008).

[45] H. Chen and C. Chan, "Transformation media that rotate electromagnetic fields," *Appl. Phys. Lett.*, vol. 90, p. 241105, (2007).

[46] W. Jiang, T. Cui, H. Ma, X. Zhou, and Q. Cheng, "Cylindrical-to-plane-wave conversion via embedded optical transformation," *Appl. Phys. Lett.*, vol. 92, p. 261903, (2008).

[47] L. Lin, W. Wang, J. Cui, C. Du, and X. Luo, "Design of electromagnetic refractor and phase transformer using coordinate transformation theory," *Opt. Express*, vol. 16, p. 6815, (2008).

[48] W. Jiang, T. Cui, X. Zhou, X. Yang, and Q. Cheng, "Arbitrary bending of electromagnetic waves using realizable inhomogeneous and anisotropic materials," *Phys. Rev. E*, vol. 78, p. 066607, (2008).

[49] J. Huangfu, S. Xi, F. Kong, J. Zhang, H. Chen, D. Wang, B.-I. Wu, L. Ran, and J. Kong, "Application of coordinate transformation in bent waveguides," *J. Appl. Phys.*, vol. 104, p. 014502, (2008).

[50] J. Li and J. B. Pendry, "Hiding under the carpet: A new strategy for cloaking," *Phys. Rev. Lett.*, vol. 101, p. 203901, Nov (2008).

[51] B. Zhang, Y. Luo, X. Liu, and G. Barbastathis, "Macroscopic invisibility cloak for visible light," *Phys. Rev. Lett.*, vol. 106, p. 033901, Jan (2011).

[52] X. Chen, Y. Luo, J. Zhang, K. Jiang, J. B. Pendry, and S. Zhang, "Macroscopic invisibility cloaking of visible light," *Nature Communications*, vol. 2, (2011).

[53] H. Chen, C. T. Chan, and P. Sheng, "Transformation optics and metamaterials," *Nature Materials*, vol. 9, pp. 387–396, MAY (2010).

[54] D. Schurig, J. B. Pendry, and D. R. Smith, "Calculation of material properties and ray tracing in transformation media," *Opt. Express*, vol. 14, pp. 9794–9804, Oct (2006).

[55] M. Rahm, S. Cummer, D. Schurig, J. Pendry, and D. Smith, "Optical design of reflectionless complex media by finite embedded coordinate transformations," *Phys. Rev. Lett.*, vol. 100, p. 063903, (2008).

[56] B. Wood and J. Pendry, "Metamaterials at zero frequency," *Journal of Physics: Condensed Matter*, vol. 19, p. 076208, (2007).

[57] A. D. Yaghjian and S. Maci, "Alternative derivation of electromagnetic cloaks and concentrators," *New Journal of Physics*, vol. 10, no. 11, p. 115022, (2008).

[58] S. Denis, L. Dusoulier, M. Dirickx, P. Vanderbemden, R. Cloots, M. Ausloos, and B. Vanderheyden, "Magnetic shielding properties of high-temperature superconducting tubes subjected to axial fields," *Superconductor Science and Technology*, vol. 20, no. 3, p. 192, (2007).

[59] F. Magnus, B. Wood, J. Moore, K. Morrison, G. Perkins, J. Fyson, M. C. K. Wiltshire, D. Caplin, L. F. Cohen, and J. B. Pendry, "A d.c. magnetic metamaterial," *Nature Materials*, vol. 7, pp. 295–297, (2008).

[60] C. Navau, D.-X. Chen, A. Sanchez, and N. Del-Valle, "Magnetic properties of a dc metamaterial consisting of parallel square superconducting thin plates," *Appl. Phys. Lett.*, vol. 94, no. 24, p. 242501, (2009).

[61] G. F. Goya, T. S. Berquo, F. C. Fonseca, and M. P. Morales, "Static and dynamic magnetic properties of spherical magnetite nanoparticles," *J. Appl. Phys.*, vol. 94, no. 5, pp. 3520–3528, (2003).

[62] F. M. Araujo-Moreira, C. Navau, and A. Sanchez, "Meissner state in finite superconducting cylinders with uniform applied magnetic field," *Phys. Rev. B*, vol. 61, pp. 634–639, Jan (2000).

Abstract

In this project we present a cylindrically symmetric device that enables magnetostatic invisibility. It can be thought as a system such that deviates magnetic fields avoiding a certain region without perturbing them outside. The design is initially based on the metamaterial concept and the mathematical technique used to characterize them: *transformation optics*. From this electromagnetic result we extract a set of permeabilities (which magnetically characterize any material) that enable magnetic cloaking. In the final part we discretize our proposal in a series of alternating layers that are already technically available. This lets us present the *antimagnet*, understood as a feasible device that makes "invisibility" achievable in the magnetostatic regime.